Cretaceous Research 176 (2025) 106199

Contents lists available at ScienceDirect

Cretaceous Research

journal homepage: www.elsevier.com/locate/CretRes

The last non-avian theropods of Europe: Palaeoecology and biogeography inferred from dental records from the uppermost Maastrichtian of Catalonia, Spain

Oscar Castillo-Visa [a,b,*], Mattia Antonio Baiano [c,d], Stephen L. Brusatte [e], Àngel Galobart [a,b], Bernat Vila [a,b]

[a] Institut Català de Paleontologia Miquel Crusafont (ICP-CERCA), Universitat Autònoma de Barcelona, Carrer de l'Escola Industrial 23, 08201, Sabadell (Barcelona), Catalonia, Spain
[b] Museu de la Conca Dellà, Carrer del Museu 4, 25650, Isona i Conca Dellà (Lleida), Catalonia, Spain
[c] Universidad Nacional de Río Negro (UNRN), Isidro Lobo 516, 8332, General Roca, Río Negro, Argentina
[d] CONICET-Área Laboratorio e Investigación, Museo Municipal "Ernesto Bachmann", Dr. Natali s/n, Villa El Chocón (Q8311AZA), Neuquén, Argentina
[e] School of GeoSciences, University of Edinburgh, Grant Institute, James Hutton Road, Edinburgh, EH9 3FE, Scotland, UK

ARTICLE INFO

Article history:
Received 4 November 2024
Received in revised form
25 June 2025
Accepted in revised form 28 June 2025
Available online 3 July 2025

Keywords:
Upper Cretaceous
Theropod palaeoecology
Systematics
Palaeobiogeography
Tooth microwear

ABSTRACT

Non-avian theropods were essential components of terrestrial ecosystems during the Mesozoic, were highly diverse in size and lifestyles across different regions of the planet. Here we assess the composition and diversity of the theropod fauna of the Ibero-Armorican island (the ancient region that encompassed present-day areas of Spain, Portugal, and France) during the final few hundred thousand years of the Cretaceous, by reviewing the theropod teeth assemblage from the locality of Molí del Baró-1 (upper Maastrichtian, C29r, Catalonia, Spain). Our study indicates a diverse fauna of small non-avian theropods with different feeding strategies and ecological niches. The tooth assemblage is significantly more diverse than previously thought and includes dental elements referred to dromaeosaurines, velociraptorines, troodontids, and an undetermined Dromaeosauridae tooth with similarities to microraptorines, as well as previously-referred teeth of cf. ?*Richardoestesia* and aff. *Paronychodon*. Microwear analysis reveals diverse feeding styles among these theropods, and particularly indicates that the troodontid had an omnivorous diet heavy in plant consumption. The assemblage of small-sized non-avian theropods and medium-to large-sized abelisaurids from the uppermost Maastrichtian of Ibero-Armorica differs from others from the European archipelago and worldwide, illustrating the high regional variability of theropod faunas around the time the asteroid impact ended the Cretaceous.

1. Introduction

Non-avian theropod dinosaurs were pivotal components of terrestrial ecosystems during the Mesozoic (e.g., Tschopp et al., 2020), spanning a wide array of taxa with varied sizes and diets that performed different roles in their ecosystems thanks to morphological specializations and unique lifestyles (Frederickson et al., 2018, and references therein). For instance, coexisting small and medium-sized non-avian theropods adopted different lifestyles without resulting in direct competition (Larson and Currie, 2013) and multiple clades of small forms successfully occupied different roles in the lower levels of secondary consumers as piscivores (Frederickson et al., 2018), small-sized predators (e.g., Torices et al., 2018), scavengers (Kane et al., 2016), and omnivores (Cullen and Cousens, 2023).

Before the end-Cretaceous extinction, in the late Maastrichtian, various groups of non-avian theropods worldwide attained large (e.g., *Rajasaurus*, *Tyrannosaurus*, Wilson et al., 2003; Horner et al., 2011, respectively), moderate (*Anzu*, *Dakotaraptor*, *Ornithomimus*, *Koleken*, *Kurupi*; Lamanna et al., 2014; DePalma et al., 2015; Claessens and Loewen, 2016; Iori et al., 2021; Pol et al., 2024, respectively), and small sizes (*Pectinodon*, *Qiupanykus*, *Trierarchuncus*, *Ypupiara*, *Tamarro*, Larson and Currie, 2013; Lü et al.,

* Corresponding author. Institut Català de Paleontologia Miquel Crusafont (ICP-CERCA), Universitat Autònoma de Barcelona, Carrer de l'Escola Industrial 23, 08201, Sabadell (Barcelona), Catalonia, Spain.
E-mail address: oscar.castillo@icp.cat (O. Castillo-Visa).

https://doi.org/10.1016/j.cretres.2025.106199

2018; Fowler et al., 2020; Brum et al., 2021; Sellés et al., 2021, respectively), and, beyond the stereotypical theropod carnivorous diet, some developed omnivory, herbivory, and highly specialist diets (Zanno and Makovicky, 2011; Funston et al., 2018; Hendrickx et al., 2019; Brum et al., 2021; Wang et al., 2024). This disparity of taxa, sizes, and diets produced distinctive microwear patterns on tooth enamel as a result of different feeding strategies, which ultimately provide insights into the ecology of the theropod assemblages. Therefore, although most of these feeding mechanisms and strategies are primarily recognizable based on the cranial structure (Barrett and Rayfield, 2006), the analysis of teeth can provide reliable data for such palaeobiological inferences. It must be taken into account, however, that non-avian theropods may have switched their ecological niches during ontogeny (e.g., Cau, 2024), especially in the case of the large-sized taxa like *Tyrannosaurus*. Traditionally, because most theropod tooth fossils are shed crowns, their isolated nature often hampered taxonomic identification beyond family level (Ösi et al., 2010; Torices et al., 2015; Marmi et al., 2016), but recent approaches based on qualitative and quantitative dental features (Hendrickx et al., 2019, 2020; Meso et al., 2021, 2022, 2024) have greatly improved their taxonomic identification. Thus, reliable taxonomic assignments of shed teeth have begun to provide crucial information on the temporal range of some theropod clades (Goswami et al., 2013) or helped to understand palaeoecological dynamics (Torices et al., 2018; Winkler et al., 2022) at the end of the Mesozoic.

In Europe, the upper Maastrichtian fossil record of non-avian theropods mainly consists of isolated teeth and fragmentary bone remains from France, Spain and Romania (Laurent, 2002; Csiki-Sava et al., 2015; Ösi et al., 2019; Pérez-Pueyo et al., 2021; Sellés et al., 2021; Isasmendi et al., 2022), which in the latest Cretaceous were part of the two main islands of the ancient European archipelago. In the largest and westernmost island, the Ibero-Armorican island (encompassing the present-day areas of Spain, Portugal, and France), the non-avian theropod record, despite being mainly based on isolated teeth and ootaxa, is diverse enough to contribute to theropod palaeobiodiversity and palaeobiogeography studies (Isasmendi et al., 2022, 2024). In the southern Pyrenees, isolated teeth (Prieto-Márquez et al., 2000; Canudo et al., 2005, 2016; Baiano et al., 2014; Torices et al., 2015; Puértolas-Pascual et al., 2018), eggs and eggshells (Vianey-Liaud and Lopez-Martinez, 1997; López-Martínez and Vicens, 2012; Sellés et al., 2014), and a few appendicular bones (Pérez-Pueyo et al., 2019; Sellés et al., 2021) have been recovered from lower and upper Maastrichtian localities. Here, we focus on the Molí del Baró-1 locality (Fig. 1), one of the uppermost Maastrichtian localities of the region, and use its theropod teeth assemblage as a case study for examining the theropod faunal composition of Ibero-Armorica at the very end of the Cretaceous, and comparing with other upper Maastrichtian localities yielding theropods from Europe and worldwide. The seven theropod shed teeth from Molí del Baró-1 include five tooth morphotypes that indicate considerable taxonomic diversity (Marmi et al., 2016), although until now their taxonomic classification has remained disputed. Our aim is to clarify the taxonomy of these teeth using quantitative and qualitative approaches, and then use this updated record to illuminate the diversity, evolution and palaeoecology of some of the last-surviving theropods of Europe.

Institutional Abbreviations: **AMNH**, American Museum of Natural History, New York, USA; **DUGF**, Delhi University, Geology Department, Fossil Catalogue, Delhi, India; **HUE**, Lo Hueco collection, housed in the facilities of Museo de las Ciencias de Castilla-La Mancha, Cuenca, Spain; **IVPP**, Institute of Vertebrate Paleontology and Paleoanthropology, Beijing, China; **LPB [FGGUB]**, Laboratory of Paleontology, Faculty of Geology and Geophysics, University of Bucharest, Bucharest, Romania; **JLUM**, Jilin University Geological Museum, Changchun, Jilin, China; **MCD**, Museu de la Conca Dellà, Isona i Conca Dellà, Catalonia, Spain; **RTMP**, Royal Tyrrell Museum of Paleontology, Drumheller, Alberta; **TMP**, Royal Tyrrell Museum of Palaeontology, Drumheller, Alberta, Canada; **UALVP**, University of Alberta Laboratory for Vertebrate Paleontology, Edmonton, Alberta, Canada; **ZPAL**, Institute of Paleobiology, Polish Academy of Sciences, Warsaw.

2. Materials and methods

Of the total sample of seven teeth from the Molí del Baró-1 locality, four partial to complete shed teeth (MCD-5033, MCD-5579, MCD-5582, and MCD-5583) from the Tremp Basin (NE Spain) were described using anatomical terminology proposed by Hendrickx et al. (2015). Photographs were taken with a Canon PowerShot SX70 HS camera, and measurements were taken directly from the images using ImageJ software. The data matrix was assembled using the software Mesquite (V3.70. Maddison and Maddison, 2019), whereas the phylogenetic analysis was carried out with the software TNT (V1.6. Goloboff and Morales, 2023). We based our analysis on the database of Meso et al. (2024), setting *Herrerasaurus* as the outgroup taxon. To run the phylogenetic analysis, we used the New Technology search algorithm with both parsimony ratchet (Nixon, 1999) and tree drifting (Goloboff, 1999) functions. The initial level of driven search was set to 30 steps, and the number of times the minimum tree length should be obtained was set to 30. Because of the high level of homoplasy and large amounts of missing data for many specimens, we summarized the most parsimonious trees using a majority rule consensus. A Principal Component Analysis (PCA) was conducted on the best-preserved teeth (MCD-5033, MCD-5582**,** and MCD-5583) using the data of Isasmendi et al. (2022). The microwear analyses were conducted with a QUANTA-250 SEM with a Ceptarus detector at the Unit from Scientific and Technological Centres (CCiTUB), Universitat de Barcelona (Catalonia, Spain), without covering the dental element surface and using the secondary electrons view. The orientation of the scratches (and especially those of the parallel to subparallel family) were determined by joining the centre of the crown apex with the equatorial section of the cervix through a straight line, defining the longitudinal plane of the crown. We find this methodology more reliable than establishing the scratches sloping relative to the carina surface, as most teeth can display a curved morphology, which often makes it difficult to recognize the scratches and their sloping.

Nomenclature Abbreviations (following Hendrickx et al., 2015) are as follow: AL (Apical Length); CA (Crown Angle); CBL (Crown Base Length); CBR (Crown Base Ratio); CBW (Crown Base Width); ce (cervix); CH (Crown Height); CHR (Crown Height Ratio); DA (Distoapical Denticle Density); DAVG (Average Distal Denticle Density); DB (Distobasal Denticle Density); DBR (Distal Denticle Base Ratio); DC (Distocentral Denticle Density); dca (distal carina); DCAL (Distal Carina Length); DDH (Distal Denticle Height); DDL (Distal Denticle Length); DDT (Dentine Thickness Distally); DDW (Distal Denticle Width); del (dentine layer); DHR (Distal Denticle Height Ratio); DLAT (Dentine Thickness Labially); DLIT (Dentine Thickness Lingually); DMT (Dentine Thickness Mesially); DSDI (Denticle Size Density Index); DSL (Distal Serrated Carina Length); enl (enamel layer); erd (eroded denticle); flu (flute); hd (hooked denticle); ids (interdenticular sulci); lad (labial flute); LAF (Labial Flutes); LIF (Lingual Flutes); lri (longitudinal ridges); MA (Mesioapical Denticle Density); MAVG (Average Mesial Denticle Density); MB (Mesiobasal Denticle Density); MC (Mesiocentral Denticle Density); MBR (Mesial Denticle Base Ratio); mca (mesial carina); MCAL (Mesial Carina Length); MCE (Mesiobasal Carina

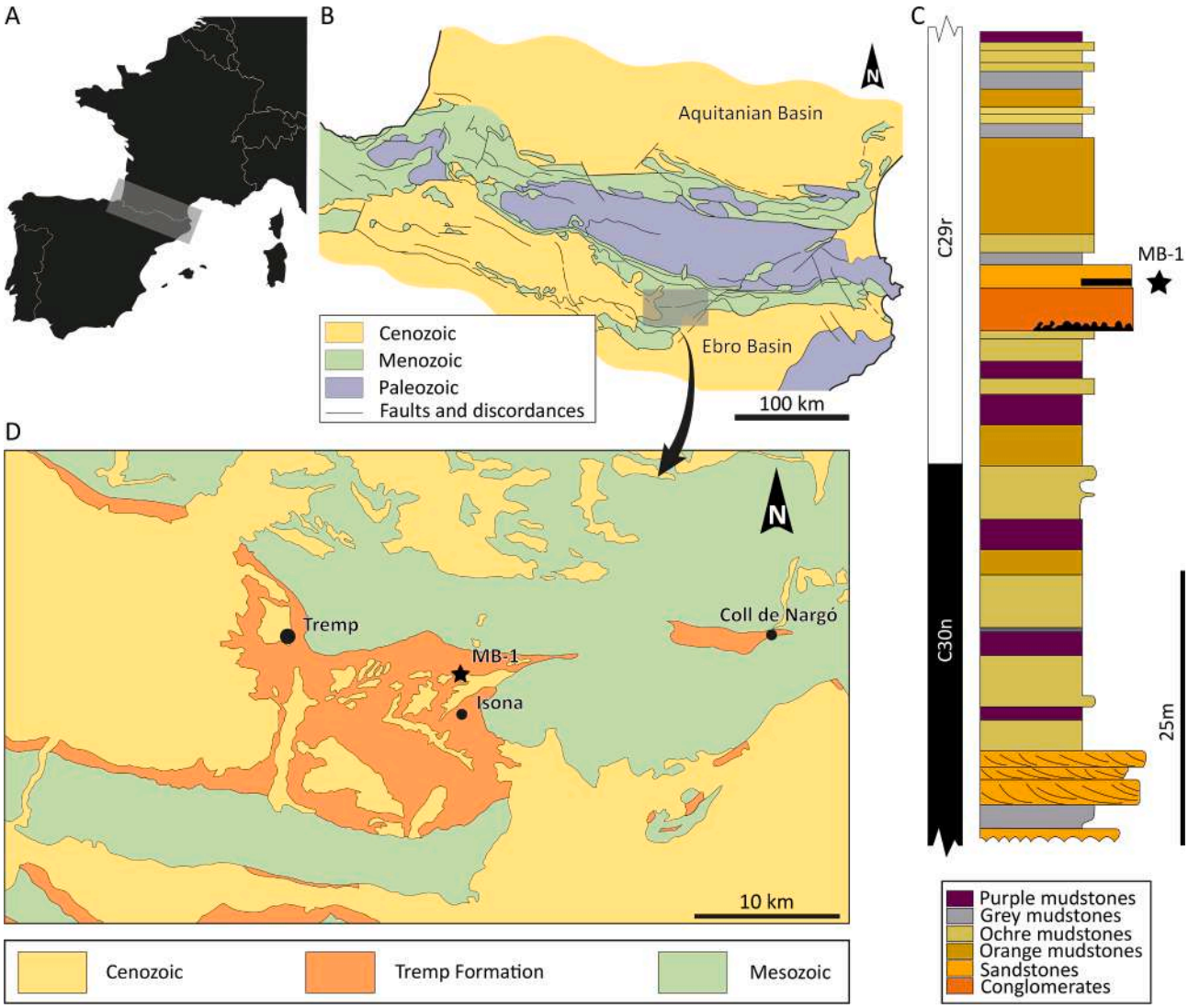

Fig. 1. Geographic and geologic situation of the Molí del Baró-1 locality, with its detailed stratigraphic section. A, Geographical map of south-western Europe. B, Geological map of the specified zone between the Ebro Basin (Spain) and the Aquitanian Basin (France), detailing the specific area of the fossil locality. C, Detailed geological map of the region, highlighting the location of the Molí del Baró-1 (MB-1) fossil locality. D, Stratigraphic section of the Molí del Baró-1 fossil locality, detailing on their left the different time frame chrons. Geological maps modified from Vissir3 (http://srv.icgc.cat/vissir3/) and Sellés et al. (2021), and the stratigraphic column was extracted and modified from Marmi et al. (2016).

Extension); MCL (Mid-crown Length); MCR (Mid-crown Ratio); MCW (Mid-crown Width); MDE (Mesiobasal Denticle Extension); MDL (Mesial Denticle Length); MDW (Mesial Denticle Width); MHR (Mesial Denticle Height Ratio); MSL (Mesial Serrated Carina Length); MUD (Marginal Undulation Density); puc (pulp cavity); sps (spalled surface); TUD (Transverse Undulation Density); tun (transverse undulation); wfa (wear facet).

3. Results

The fossil locality of Molí del Baró-1 corresponds to the fluvial deposits of the Talarn Formation or 'Lower red Garumnian' unit of the Tremp Group (C29r magnetochron, late Maastrichtian; Fondevilla et al., 2019). Molí del Baró-1, discovered in 2001 and excavated during five seasons (2002, 2007, 2010, 2011, and 2023), is one of the richest fossil localities in the Tremp Basin (Marmi et al., 2016), with a high diversity of vertebrates (mainly shed teeth, bones, and eggshells of dinosaurs and crocodylomorphs), invertebrates (mollusc shells, partial insect exoskeletons, and eggs), and plants (charophytes, sporomorphs, angiosperm leaves, seeds, and logs).

To date, seven shed teeth have been described at the locality (Marmi et al., 2016), four of which we review here. They are represented by partial to complete shed teeth of small size (<1 cm in apicobasal length), and three of them preserve only the crown, whereas the other one also preserves the root. The teeth display some cracking, usually sliced in sections, and lack parts of the carinae or some denticles. However, they are preserved well enough that we can discern their taxonomic assignment.

3.1. Systematic palaeontology

DINOSAURIA Owen, 1842
SAURISCHIA Seeley, 1888
THEROPODA Marsh, 1881
TETANURAE Gauthier, 1986
COELUROSAURIA Von Huene, 1914
MANIRAPTORA Gauthier, 1986

PARAVES Sereno, 1997
DROMAEOSAURIDAE Matthew and Brown, 1922
VELOCIRAPTORINAE Barsbold, 1983

MCD-5033 is a ziphodont tooth that preserves both the crown and the root, although the latter lacks its distal portion (Fig. 2A, B). The tooth is fragmented close to the cervix, and the mesial part of the cervix and carina are lost in this region. The crown is highly depressed labiolingually (MCW = 1.45 mm), especially in the medial part, resulting in an 8-shaped cross-section (Fig. 2C); this constriction is also observed in the root, although less pronounced. Along its height, the crown is slightly sinuous, curved lingually and labially, and apicobasally higher than mesiodistally long (CHR = 1.91; Fig. 2D). The tooth is curved distally, with the mesial carina having a lower slope than the distal one. At the cervix, the boundary between the root and the crown is irregular, shifting apicobasally through the mesiodistal plane of the tooth (Fig. 2B). Additionally, there is no constriction between the root and the crown.

The ornamentation of the crown surface consists of slightly sculptured enamel with braided ridges oriented mesioapically close to the mesial carina. The ornamentation is not extended to the denticles of the mesial and distal carinae (Fig. 2E), despite it being only present in the basal third of the crown. The crown shows multiple faintly marked transverse undulations on the enamel (only appreciable when a light source is applied over the crown surface at a low angle; Fig. 2E). The carinae along the crown show some displacements. The base of the mesial carina is slightly displaced lingually and opposes apically, labially near the apex, creating a sinuous projection (Fig. 2F). The distal carina is centrally positioned, curving lingually close to the base of the crown in distal view (Fig. 2G). Denticles on the distal carina show a progressive shift from a subrectangular shape at the base to subquadrangular apically (Fig. 2B, D, and E). Also, their size (DDH = 0.20 mm; DDL = 0.15 mm) increases apically and consequently the denticle density decreases (DB = 38.75; DC = 35; DA = 32.5 denticles/5 mm). Only the apicalmost denticles are slightly apically tilted. These denticles are relatively deep mesiodistally, whereas they are labiolingually wider than long apicobasally, and apically they become wider progressively. Their interdenticular space is restricted although the inner part seems to be wider, forming a slight tear-drop shape and connecting to a short interdenticular sulcus (Fig. 2C). The distal interdenticular slits seem to become deeper in the mid-crown denticles.

Denticles of the mesial carina (present along all the carina. Fig. 2B, D) are subcircular and smaller than the distal ones (MDL = 0.13 mm), despite showing the same size apically. The interdenticular spaces are clearly reduced compared to the distal denticles, but the interdenticular slits seem to be similar along the carina until reaching the crown apex. Contrary to the distal carina, the apical mesial denticles are the smallest ones (Fig. 2D). MB = 41; MC = 37.5; MA = 45 denticles 5 mm (see MCD-5033 Supplementary Measurements). Both distal and mesial denticles develop operculums, which represent over 20–25 % of total denticle height.

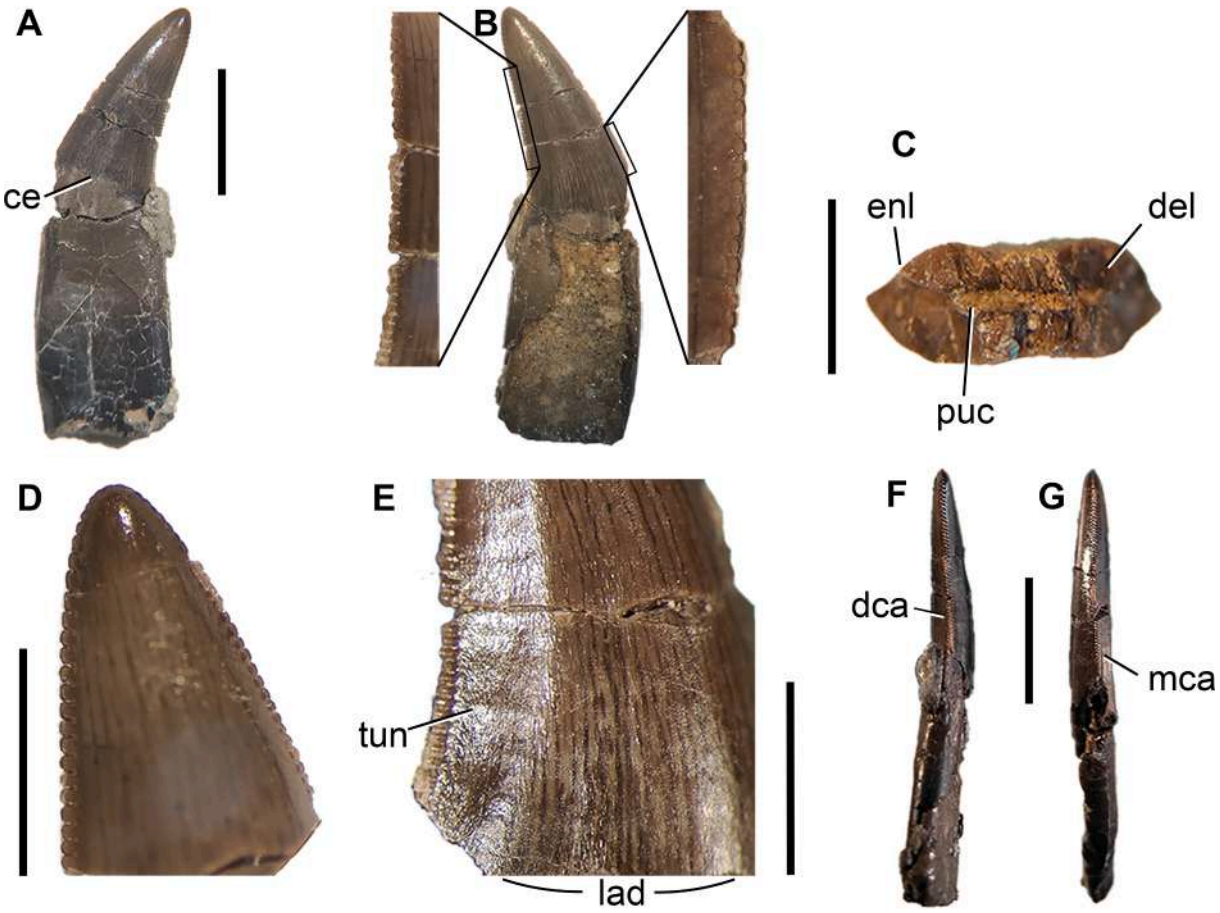

Fig. 2. Tooth MCD-5033. A, tooth in lingual view; B, tooth in labial view with close-up images of the denticles at the distal (left) and mesial (right) carinae; C, cross-section of the tooth near the cervix; D, Detail of the crown, showing the crown apex and the apical denticles; E, close-up view of labial view showing the wide labial depression and the transverse undulations; F, tooth in mesial view; G, tooth in distal view. Abbreviations in the text. Scale bars equal 5 mm in A, B, F, G, and 2 mm in C, D, and E.

The apical zone of the crown does not show any wear or spalled surface (Fig. 2D). On the crown apex, the denticles seem to be eroded.

MCD-5033 was assigned by Marmi et al. (2016) to Theropoda indet. based on the absence of significant features, although the authors underscored its affinities to *Richardoestesia* due to their small size. The present review of the specimen recognizes MCD-5033 as a lateral tooth of Velociraptorinae based on the combination of the following dental features proposed by Hendrickx et al. (2019) for this clade: 1) presence of a ziphodont dentition with serrated mesial and distal carinae in at least some lateral teeth; 2) lateral tooth with ridged carinae; 3) absence of a constriction between the root and the crown base; 4) a strongly concave distal margin; and, 5) an 8-shaped cross section of the crown base. It is worth noting that features 3 and 4 are considered unambiguous synapomorphies for Dromaeosauridae, whereas feature 5 is present in all velociraptorines other than *Deinonychus* (Hendrickx et al., 2019).

Our review of MCD-5033 suggests some resemblance to the teeth assigned to *Richardoestesia* and *Velociraptor*, as also underscored by the PCA analysis (see below). However, MCD-5033 differs from *Richardoestesia gilmorei* teeth (with *R. gilmorei* being more similar to MCD-5033 than *R. isosceles*) described by Larson (2008), Hendrickx and Mateus (2014), and Isasmendi et al. (2022), in the following features: display of a braided enamel instead of a smooth or irregular texture; development of an 8-shaped outline in cross-section; the presence of a long crown height (CH) of 9.65 mm, this value being higher than recorded in the Laño and Alberta teeth of *R. gilmorei* (between 1.37 and 6.82 mm. Larson, 2008; Isasmendi et al., 2022); development of transverse undulations and lack of longitudinal ones, whereas *Richardoestesia* displays the opposite case; and maybe the lingual displacement and sinuous projection of the carinae. Most of these features are present in the teeth of some velociraptorines (Sweetman, 2004). Consequently, MCD-5033 is reclassified here as an undetermined Velociraptorinae tooth.

The tooth MCD-5033, assigned to Velociraptorinae, resembles the specimen HUE-10051 from the Campanian-Maastrichtian site of Lo Hueco (Cuenca, Spain; Ortega et al., 2015; Fig. 3B). Both teeth have a similar curved morphology, a depressed medial section, and serrated mesial and distal carinae (where denticles in the distal carina increase in size apically). However, these teeth have numerous differences: the mesial surface of HUE-10051 starts to tilt distally more apically than MCD-5033 (Fig. 3A and B); the apical part of the mesial surface is also more curved (Fig. 3A and B); it lacks transverse undulations; the mesial carina seems to bear denticles only on the apical region; denticle density (2.5–6 denticles/mm) is lower than in MCD-5033 (7–8 denticles/mm); denticles have a slight hooked shape (and not sub-quadrangular at distal carina or subcircular at mesial one as observed in MCD-5033); and the apex seems to be more pointed than in MCD-5033.

We here make comparisons between MCD-5033 and other dromaeosaurid teeth from the global Cretaceous. ZPAL MgD-I/97 is an isolated ziphodont tooth of *V. mongoliensis* that bears serrated mesial and distal carinae (Fig. 3C; Barsbold and Osmólska, 1999). However, the apical region of the crown in ZPAL MgD-I/97 is less distally projected than in MCD-5033. The Mongolian specimen has larger denticles, and consequently it has a lesser denticle density in both carinae (around 7 denticles/mm in mesial carina and over 5 denticles/mm in distal carina), whereas the Molí del Baró-1 specimen has 9 and 6.5 denticles/mm, respectively (Supplementary Material). On the distal carina, both teeth display smaller but more numerous denticles in the basal region, increasing in size apically (Fig. 3A, C). MCD-5033 shares similarities with a Velociraptorinae tooth (UALVP 50531, Fig. 3D) from the uppermost Santonian Milk River Formation of Alberta, Canada (Larson, 2008). The ziphodont curved morphology, the presence of a longitudinal median depression, the labiolingual compression, a distal carina reaching a basally displaced cervix, distal denticles being bigger than mesial ones, and a blunted crown apex are characters that of UALVP 50531 shares with MCD-5033. Also, UALVP 50531 might have transverse undulations like MCD-5033. Conversely, UALVP 50531 has larger distal denticles, which are lower in number than in MCD-5033, and they are slightly hooked, whereas the mesial ones are sub-rectangular, traits that differ from MCD-5033.

Furthermore, the dromaeosaurid tooth LPB [FGGUB] R.2289 described by Csiki-Sava et al. (2016) (Fig. 3E) from the upper Maastrichtian levels of the Haţeg Basin (Romania) is vaguely similar to MCD-5033. Its crown has a curved shape, serrated distal and mesial carinae (with the distal denticles being larger than the mesial ones), the presence of some faint transverse undulations, and possibly a labial depression. The crown is proportionally shorter than that of MCD-5033, the distal denticles of the Romanian specimen are larger and lower in number than those of MCD-5033, and the mesial denticles apparently are only present at the apical half of the crown, unlike the Catalan specimen. Also, Csiki and Grigorescu (1998) reported a Velociraptorinae tooth crown (LPB [FGGUB] R.1428) from the upper Maastrichtian "La Carare" locality (Haţeg Basin, Romania). Although LPB [FGGUB] R.1428 is incomplete (Fig. 3F), the mesial and distal carinae pattern in the crown is similar to that of MCD-5033. Moreover, LPB [FGGUB] R.1428 also has a pronounced labial depression. The distal denticles resemble those of MCD-5033 but differ in that the mesial carina holds denticles only in the apical half of the crown. MCD-5033 shows a similar mesial carina to the Dromaeosaurinae tooth TMP 2009.136.0008, described by Larson et al. (2010) from the lower Maastrichtian Horseshoe Canyon Formation of Canada (Fig. 3G). In addition, TMP 2009.136.0008 has subquadrangular distal denticles (*sensu* Hendrickx et al., 2015), similar to the apicodistal denticles of MCD-5033. However, TMP 2009.136.0008 presents smaller interdenticular slits and a more pronounced interdenticular space. Finally, MCD-5033 and *Velociraptor mongoliensis* IGM 100/1252 (Turner et al., 2007) share smaller denticles on the mesial carina compared to those of the distal carina, but a wider comparison is not possible due to the lack of a detailed description of the Mongolian material in the literature.

DROMAEOSAURIDAE Matthew and Brown, 1922

DROMAEOSAURINAE Matthew and Brown, 1922

MCD-5583 is a ziphodont tooth with the crown and part of the root curved lingually (Fig. 4). The cervix is well preserved, but part of the crown apex and the base of the distal carina are lost (Fig. 4A, B). This carina is concave in the apical half (Fig. 4A) and curved labially (Fig. 4C).

The mesial surface is fairly distally inclined, whereas the distal carina still points apically, and it is only displaced distally in the crown apex (Fig. 4A, B). This could indicate that this tooth occupies a mesial position in the tooth row. The labial surface is mostly flat, or even slightly concave (Fig. 4C); however, the lingual surface is clearly convex (Fig. 4C). There is no constriction between the crown and the root. The basal cross-section has a 'J' outline (Fig. 4F). Dentine comprises most of the tooth thickness, and the pulp cavity is reduced, developing a hollow space with a conical outline. The dentine displays a radiated, fibered texture in the mesial region.

The mesial carina is unserrated near the base and at mid-height of the crown. Apically, we cannot estimate the presence of

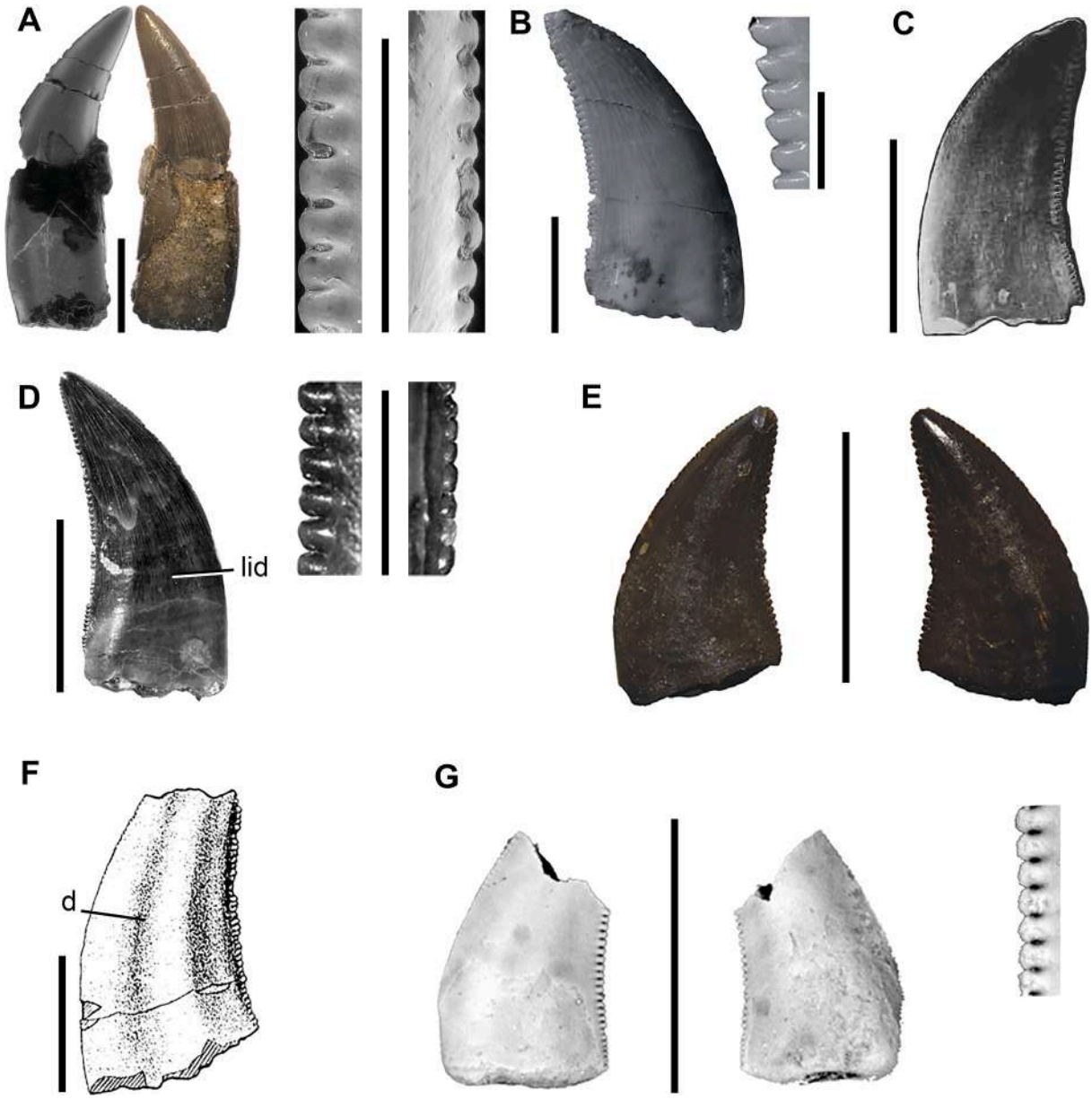

Fig. 3. Morphological comparison of MCD-5033 (Velociraptorinae) tooth similar teeth. A, MCD-5033 (from left to right: lingual view (SEM image), labial view, distal carina denticles (SEM), and mesial carina denticles (SEM); B, HUE-10051 (Velociraptorinae) tooth on lateral view and a detail of their mid-high denticles (extracted and modified from Ortega et al., 2015); C, ZPAL MgD-I/97a (*Velociraptor*) tooth in lateral view (extracted and modified from Barsbold and Osmólska, 1999); D, UALVP 50531 (Velociraptorinae) tooth in lateral view and details of their distal and mesial denticles, respectively (extracted and modified from Larson, 2008); E, LPB [FGGUB] R.2289 (Dromaeosauridae) tooth crown in lingual and labial views (extracted and modified from Csiki-Sava et al., 2016). F, LPB [FGGUB] R.1428 (Velociraptorine) tooth crown drawing in lateral view (extracted and modified from Csiki and Grigorescu, 1998); G, TMP 2009.136.0008 (Dromaeosaurinae) tooth in lateral views and detail of their distal denticles (extracted and modified from Larson et al., 2010). Abbreviations in the text. Scale bars equal 5 mm in all figures, except for close-up images of denticles (1 mm; G is not to scale).

denticles due to a wear facet (Fig. 4D). The distal carina is lingually displaced near the cervix, whereas it is medially centered near the apex. This carina holds poorly preserved large denticles (Fig. 4E, H), which decrease in size apically. Denticles are labiolingually wider than apicobasally tall (DBR = 1.42; see Supplementary Material for expanded data). They are tilted, point apically (Fig. 4H), and remain straight independently of the distal carina curvature in the apical region. Most of the denticles, especially those situated at mid-height, have short and poorly marked interdenticular sulci. The interdenticular space increases apically (at least in the basal-middle denticles, from 0.11 mm to 0.19 mm. See MCD-5583 Supplementary Measurements). Opercula are not observable, maybe due to the worn state of the denticles (Fig. 4H).

The labial and lingual surfaces bear four to five longitudinal faint ridges (Fig. 4D), especially concentrated in the mesial part, that end near the cervix. On the labial surface, there are three or four barely visible transverse undulations (Fig. 4E). MCD-5583 develops a braided enamel texture on the basal surface in the distal region of the crown and a smooth one on the mesial surfaces. The presence of wear facets, spalled surfaces, resorbed roots, and eroded denticles (Fig. 4A-G, H) might indicate that MCD-5583 was a shed tooth (based on Currie et al., 1990).

The specimen MCD-5583, previously identified as an indeterminate Theropoda (Marmi et al., 2016) and later as cf. *Arcovenator* (Fondevilla et al., 2019), is here recognized as a tooth from the mesial part of the snout and assigned to an indeterminate

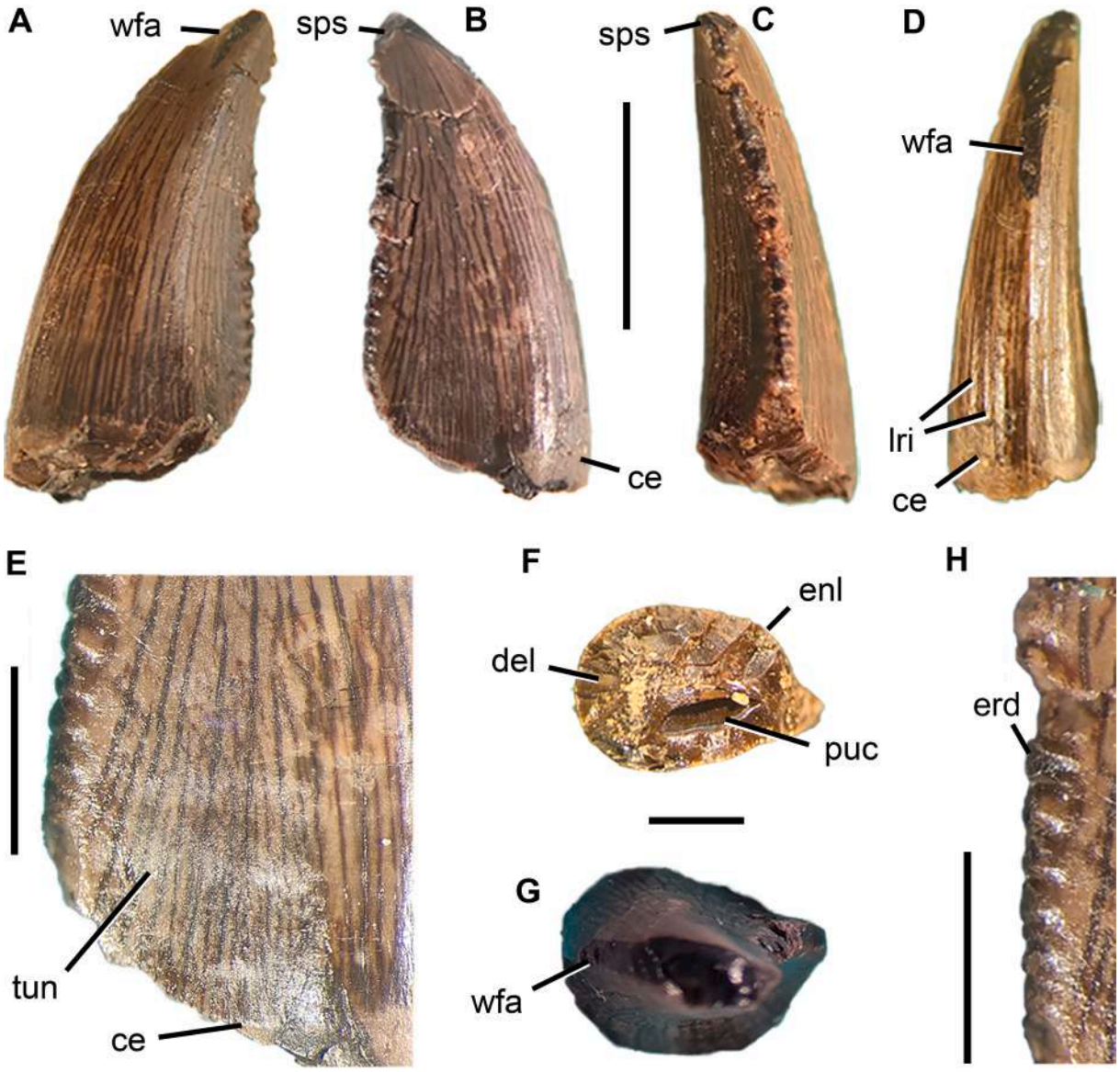

Fig. 4. Tooth MCD-5583. A, tooth in lingual view; B, tooth in labial view; C, tooth in distal view; D, tooth in mesial view; E, labial view detail with transverse undulations (tun) over the crown; F, basal cross-section; G, tooth in apical view; H, distal carina detail with the most complete denticles. Abbreviations in the text. Scale bars equal 5 mm in A to D, and 2 mm in E to H.

Dromaeosaurinae. The new assignment is based on the presence of a J-shaped cross-section of the crown base, which is considered an unambiguous synapomorphy of Dromaeosauridae (Hendrickx et al., 2019), and a dental feature of Dromaeosaurinae.

The MCD-5583 tooth, attributed to Dromaeosaurinae, has some resemblance to HUE-10052, a Dromaeosaurinae tooth from the Campanian-Maastrichtian Lo Hueco fossil site in Spain (Ortega et al., 2015). Both teeth are similar in shape (Fig. 5A and B), ziphodont, and have straight crowns. They also share a barely curved distal carina, and a convex mesial margin, a concave depression near the distal carina, and a similar distal denticle density (2.5 denticles per millimeter; Supplementary Material).

We here make comparisons between MCD-5583 and other dromaeosaurid teeth from the global Cretaceous. Currie et al. (1990) described a *Saurornitholestes langstoni* tooth (TMP 82.16.43) from southern Alberta (Judith River Formation, Canada) that is similar to MCD-5583 (Fig. 5C). It has a barely curved, serrated distal carina (although with numerous small-sized denticles) and a lingually twisted and unserrated mesial carina. The *S. langstoni* tooth shows a deep wear facet on the labial surface, differing from the mesial wear facet of MCD-5583. The specimen TMP 82.16.43 is labiolingually narrower than MCD-5583, and its crown is more straight compared to the labially curved crown of MCD-5583. MCD-5583 is also morphologically similar to RTMP 87.83.1, a *Saurornitholestes* sp. tooth from the Late Campanian Judith River Group, Alberta (Sankey et al., 2002). Both teeth have a very similar denticulated distal carina with relatively large denticles and a J-shaped cross-section of the crown base (*sensu* Hendrickx et al., 2015; Fig. 5A, D). However, the Canadian tooth has a lingually displaced mesial carina, lacks longitudinal flutes on the mesial surface, and has wear facets in the apical region.

DROMAEOSAURIDAE Matthew and Brown, 1922
Dromaeosauridae indet.

MCD-5582 is a ziphodont tooth that preserves most of the crown, except the apex and the base of the distal carina (Fig. 6A, B).

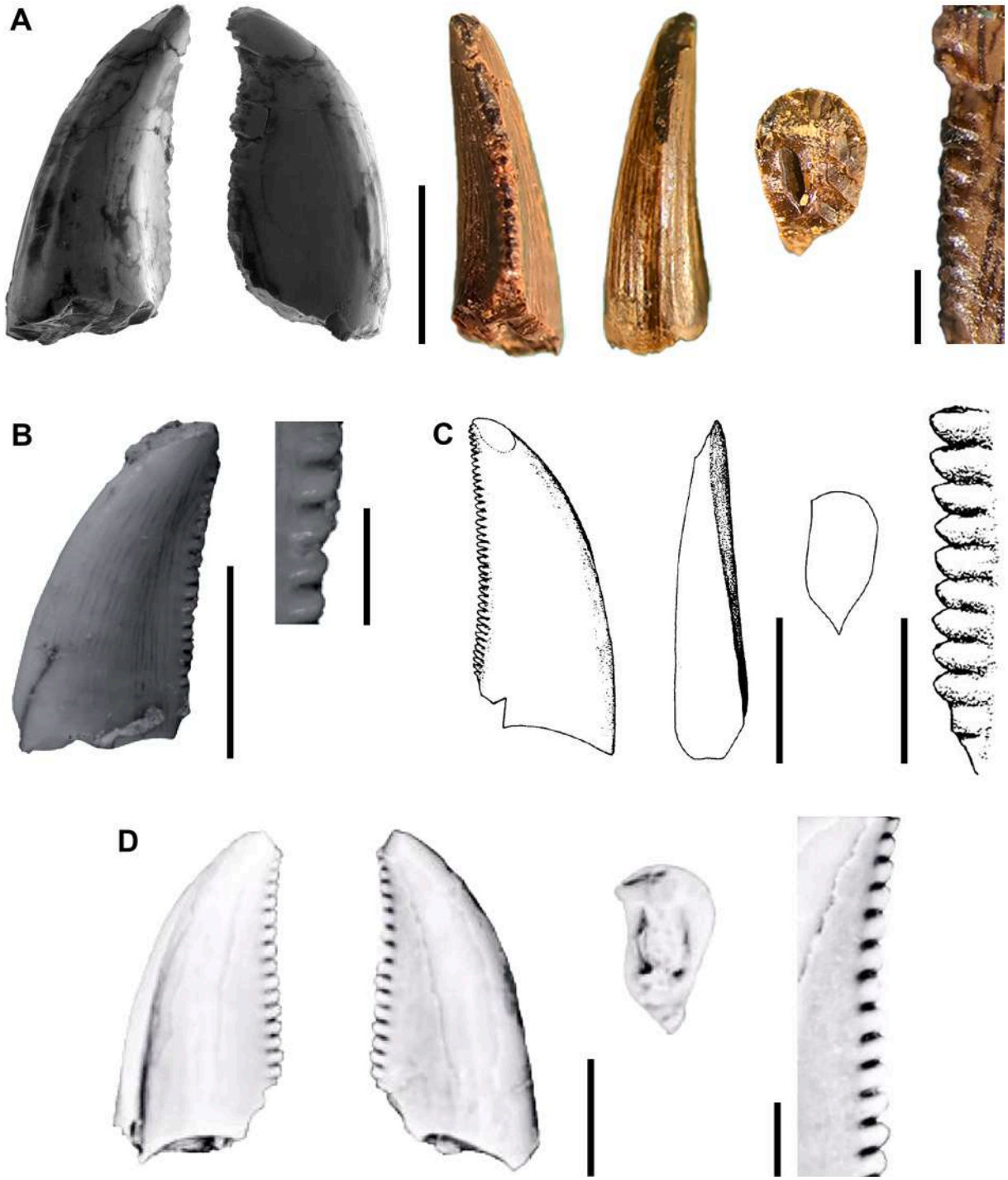

Fig. 5. MCD-5583 (Dromaeosaurinae) tooth and similar teeth. A, MCD-5583 (from left to right: lingual and labial (SEM) views, distal view, mesial view, cross-section and distal carina denticles). B, HUE-10052 (Dromaeosaurinae) tooth in lateral view and a detail of their mid-high denticles (extracted and modified from Ortega et al., 2015); C, TMP 82.16.43 (*Saurornitholestes langstoni*) drawing on labial, mesial and cross-section views, and details of the distal denticles (extracted and modified from Currie et al., 1990); D, RTMP 95.92.28 (*Saurornitholestes* sp.) tooth crown in lateral and cross-section views, and details of the distal denticles (extracted and modified from Sankey et al., 2002). Scale bars equal 5 mm for all figures, except for close-up images of denticles (1 mm).

The distal carina is apparently broken at the contact with the root, along the cervix. In mesodistal view, the tooth is highly compressed labiolingually (MCW = 1 mm; Fig. 6C), showing a sigmoidal curvature (Fig. 6C). In labial view (Fig. 6B), the tooth is slender, having a slight curvature apically. No wear facets are preserved on the labial or lingual surfaces. Along the crown's lower half, there is a slight but visible lingual depression (Fig. 6A, F). The crown's surface near the cervix is compressed on the mesial and labial margins (Fig. 6C, D), and the basal cross section has a parlinon outline (*sensu* Hendrickx et al., 2015, and references therein. MCR = 0.64; Fig. 6G).

MCD-5582 lacks denticles on the mesial carina and the apical half of the distal carina. In general, both carinae consist of a smooth and thin ridge, and they are moderately expanded in the

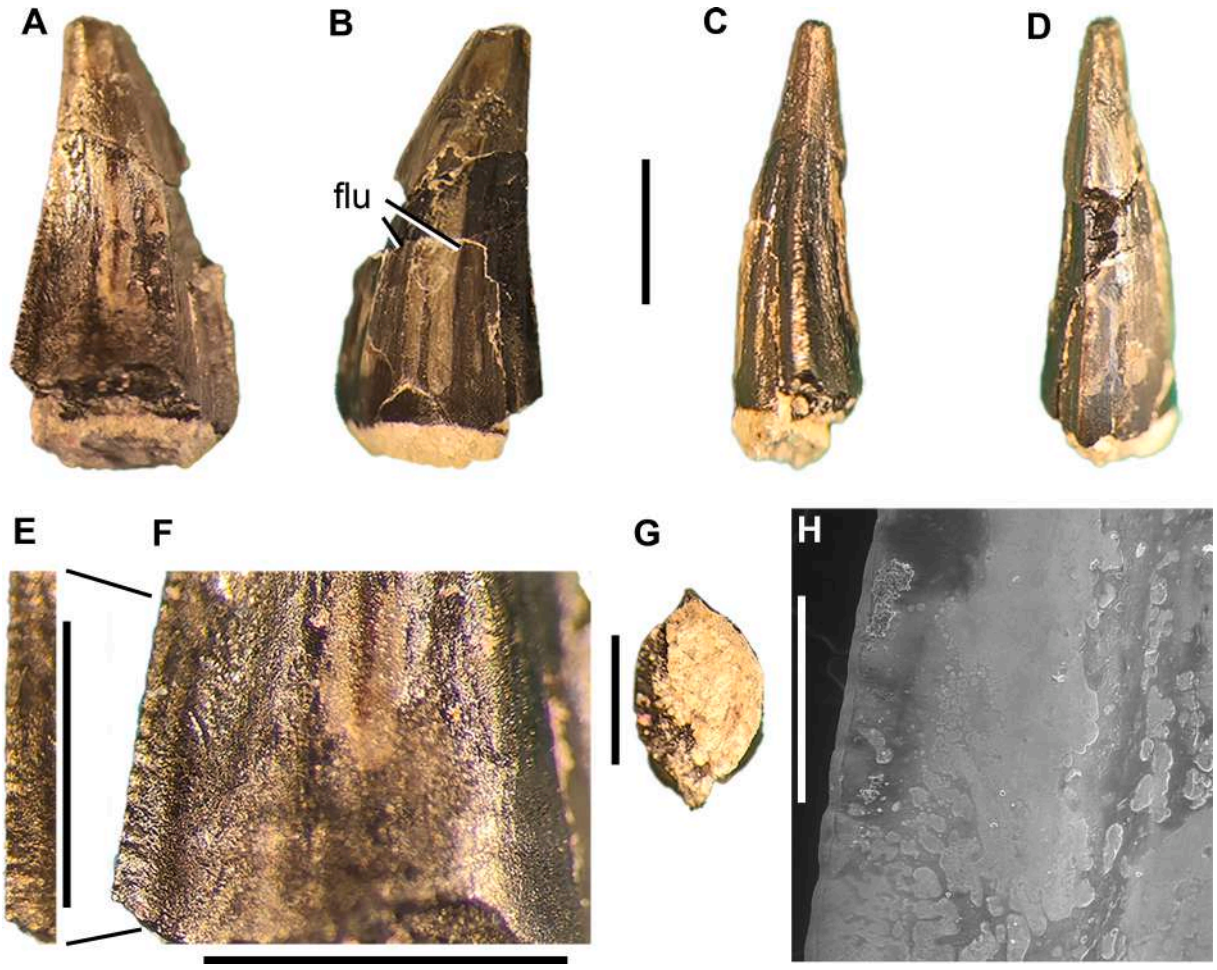

Fig. 6. Tooth MCD-5582. A, tooth in lingual view; B, tooth in labial view; C, tooth in distal view; D, tooth in mesial view; E, detail in lingual view of the crown in lingual view showing the enamel's texture, the lingual depression, and the minute distal denticles; F, Tooth crown base at lingual view, also showing the basal part of the distal carina; G, cross-section of the tooth (mesial carina pointing upside); H, SEM image of the distal carina lingual surface showing the denticles. Abbreviations in the text. Scale bars equal 2 mm in A to F, and 500 μm in G.

mesiodistal plane. The carinae are slightly displaced lingually (Fig. 6C, D, and F), but they are almost straight apicobasally with a slight curvature. The mesial carina is mesially developed and, in the basal region, seems to reach the cervix (Fig. 6A, B, and D). The lingual margin of this carina is depressed, forming a concave surface, whereas in the labial margin the depression is distally displaced andless pronounced. Also, the anterior margin of the labial surface has the same concave curvature as the depression on the lingual surface, increasing its thickness on the labial surface. On the other hand, the mesial carina is convex labially, whereas the distal one is straight (or slightly convex) labially.

As mentioned above, tiny denticles are only present on the distal carina, which is located from the cervix to mid-height of the crown and turns smaller apically (Fig. 6E, H. See MCD-5582 Supplementary Measurements). These denticles are labiolingually thin (DDW = 0.13 mm), mesiodistally longer than apicobasally tall (DBR = 0.84), and their shape is barely recognizable, but they seem to be subquadrangular in labiolingual view (Fig. 6H), as in *Suchomimus* (Hendrickx et al., 2015, Fig. 8E). No operculum is observed. The interdenticular slits between denticle ends are short; the interdenticular diaphysis is also difficult to recognize; and the interdenticular sulci are absent.

Regarding tooth ornamentation, MCD-5582 displays multiple shallow longitudinal ridges on the labial and lingual surfaces (four on the labial surface and three on the lingual one. Fig. 6A, B). No transverse undulations are observed, and the enamel texture seems to be composed of circular and irregular pits that might be produced by taphonomic processes, but in general the texture is irregular, with some sub-straight striations close to carinae (Fig. 6F).

Due to the moderately curved mesial carina, the nearly straight projection of the distal carina in lateral view, and the relatively thin labiolingual section (Fig. 6A-F), we consider MCD-5582 as a mesial tooth (also see Maranga (2021), as crown morphology seems to change along the mesial position).

MCD-5582 was originally classified as *?Euronychodon* (Marmi et al., 2016) based on the lack of denticles, the development of two longitudinal flutes, and the general shape of the crown. In the present PCA analysis, MCD-5582 falls in the Dromaeosauridae morphospace. However, this tooth shares morphological similarities and dental features with Lower Cretaceous microraptorines, such as: 1) a Crown Base Ratio (CBR) higher than 0.64 (Fig. 6A, B); 2) relatively short crown; 3) concave surface adjacent to carinae (Fig. 6A-D, F); 4) twisted mesial carina (Fig. 6D); 5) displaced distal carina; 6) absence of hooked denticles (Fig. 6E, F); 7) absence of convex distal margins (being concave in the current specimen); 8) absence of transverse and marginal undulations (Fig. 6A, B, E); 9) smooth or irregular tooth surface texture (Fig. 6E, F); 10)

longitudinal ridges in mesial teeth (Fig. 6A, B). Additionally, constricted crowns in the cervix with unserrated mesial carina are typical dental features of microraptorine teeth; although Hendrickx et al. (2019) mention this trait as present in lateral positions, it is also noticed in the microraptorine mesial teeth (Xu and Li, 2016; Maranga, 2021). Finally, the assignment of MCD-5582 to *Paronychodon* (considering *Euronychodon* as a *nomen dubium* taxon *sensu* Rauhut, 2002; Torices et al., 2015) is unlikely due to the absence of the typical curved distal carina, the lack of a flattened lingual surface, and the presence of denticles (Currie et al., 1990; Sankey et al., 2002; Sues and Averianov, 2013; Torices et al., 2015).

MCD-5582 (Fig. 7A), herein assigned to Dromaeosauridae indet., shares remarkable morphological similarities and dental features with Lower Cretaceous microraptorines, and this prompts us to compare it with various tooth morphotypes of this clade. For instance, we focus on an indeterminate Microcraptorinae (JLUM Y-MR160501) with a near-complete dental series from the Aptian sediments of the Jiufotang Formation (China, Maranga, 2021). In particular, MCD-5582 resembles the fourth (and vaguely the second) maxillary teeth of JLUM Y-MR160501 (Fig. 7B). The fourth maxillary tooth of the mentioned Chinese specimen shares with MCD-5582 a poorly posteriorly recurved ziphodont morphology, an unserrated mesial carina but a serrated distal carina, the presence of longitudinal ridges, a labial surface that is labially expanded, and the development of a constriction between root and crown. MCD-5582 is also similar to the sixth premaxillary tooth of IVPP V 13476, a Lower Cretaceous indeterminate microraptorine from the Jehol Group (China, Xu and Li, 2016). Like the Molí del Baró-1 tooth, the crown of the IVPP V 13476 tooth is slightly curved distally in labial view (Fig. 7C), with its mesial carina apically increasing their convex curvature more pronouncedly than the distal carina. The mesial carina lacks denticles, and the distal one contains numerous small-sized denticles (like MCD-5582). Also, both dental elements seem to be labially expanded. However, both teeth preserve a constriction between root and crown, being a trait clearly more pronounced in MCD-5582.

PARAVES Sereno, 1997
TROODONTIDAE Gilmore, 1924 *sensu* Turner et al., 2012

MCD-5579 is a lateral, ziphodont tooth that only preserves the crown, lacking the crown apex (Fig. 8). The crown surface is affected by cracks and fissures, but most of its morphological features are recognizable. The crown is relatively short (with CBL measuring at least 4.5 mm, Fig. 8A-B; Supplementary Material) and slightly curved lingually, and is apicobasally higher than mesiodistally long (CHR = 1.20). Further, it is relatively labiolingually wide (CBR = 0.49) and has a denticulated distal carina (Fig. 8C), but lacks a mesial one. The tooth shows an outline with a pronounced distal curvature in labial and lingual views, the mesial surface being much more curved than the distal one. The cervix is not well preserved, and it is only possible to infer that there was no constriction between root and crown (Fig. 8A-B, D-E). Crown surface ornamentation is composed of a slightly marked, braided texture oriented apicobasally on most of the surface, whereas the surfaces adjacent to the distal carina show an irregular texture (Fig. 8F). No transverse undulations are appreciable on the crown surface. There are two subtle longitudinal flutes, one on each side and mesially located (Fig. 8E, G).

The distal carina in MCD-5579 is apicobasally straight and slightly displaced labially (Fig. 8D). Both lingual and labial surfaces are concave when adjacent to the distal carina (Fig. 8A). This concavity starts to develop at the labiolingually widest section of the crown. No marginal undulations are observed.

Recorded denticles are proportionally large (DDH = 0.39 mm; DDL = 0.33 mm) and low in number (total number of preserved denticles = 9) primarily due to their size. Apical denticles are not preserved, and only a portion of the basal and middle denticles are present (Fig. 8C-D, H). Their density diminishes apically (DB = 17.5; DC = 15 denticles/5 mm), suggesting an increase in size apically or an increase the denticle interdenticular spaces. The denticles are characteristically hook-shaped (Fig. 8C), slightly apically directed, and as apicobasally long as labiolingually wide (DBR = 0.99. Fig. 8D. See MCD-5579 Supplementary Measurements). Close to the apex, the denticles are slightly labiolingually thinner. The distalmost part of the well-preserved denticles bears a very thin operculum. Because denticles are hooked-shaped, their interdenticular slits are pronounced (Fig. 8C), having constrained interdenticular spaces that connect to short interdenticular sulci. Pits are only found around the distal carina; most of them are concentrated on its basal part, and a few are present over denticles.

Marmi et al. (2016) classified MCD-5579 as Dromaeosauridae indet. based on its distally recurved and labiolingually compressed crown, a teardrop-shaped cross-section of the crown base, a serrated distal carina, the lack of a mesial carina, and the presence of asymmetrical and apically pointed denticles, which are distalloapically oriented and have a marked constriction at their bases. Here, we instead regard it as a Troodontidae lateral tooth based on the combination of the following dental features

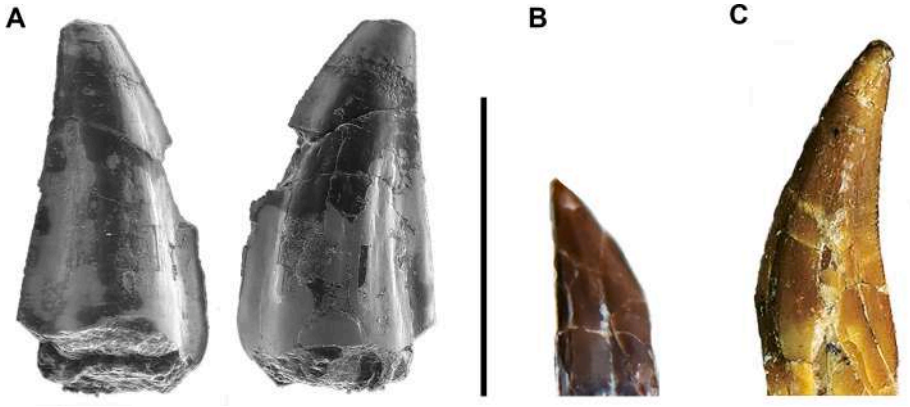

Fig. 7. MCD-5582 (Dromaeosauridae indeterminate) tooth and similar teeth. A, MCD-5582 on lingual and labial (SEM) views; B, JLUM Y-MR160501 (Microraptorine) tooth outline in labial view (extracted and modified from Maranga, 2021); C, IVPP V 13476 (Microraptorine) tooth in labial view (extracted and modified from Xu and Li, 2016). Scale bars equal 5 mm.

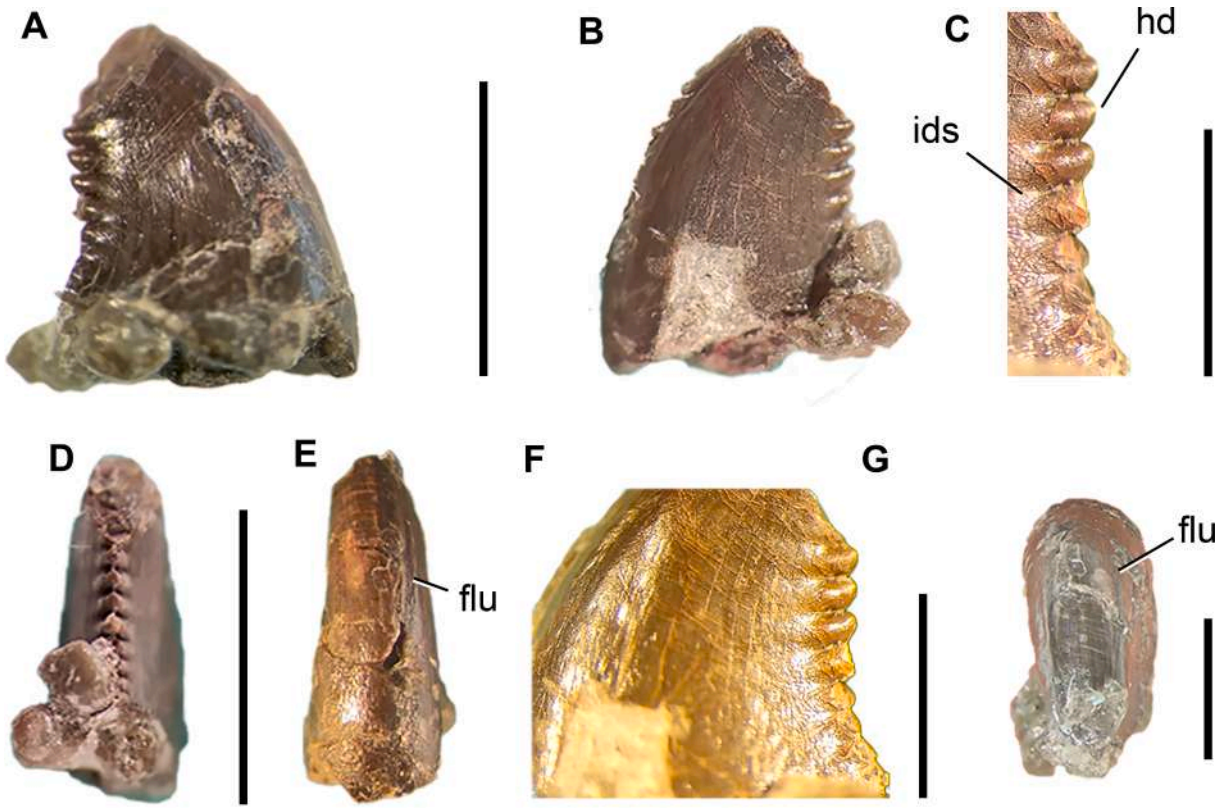

Fig. 8. Tooth MCD-5579. A, tooth in lingual view; B, tooth in labial view; C, detail of the distal denticles in labial view; D, tooth in distal view; E, tooth in mesial view; F, close-up image in labial view and details of the crown's enamel texture; G, tooth in apical view. Abbreviations in the text. Scale bars equal 5 mm in A, B, D, and E, and 2 mm in C, F, and G.

(recognized by Hendrickx et al., 2019): 1) relatively short crown height; 2) unserrated mesial carina (i.e. Norell et al., 2009); 3) concave surface adjacent to the carinae; 4) distal carina centrally positioned or slightly displaced (crown sub-symmetrical); 5) small number of large distal denticles (i.e., fewer than 15 denticles/5 mm. See Larson and Currie, 2013); 6) hook-shaped denticles (i.e. Makovicky et al., 2003); 7) absence of marginal undulations; and 8) presence of interdenticular sulci and transverse undulations (as in *Troodon*). Because of its incompleteness, no we did not include MCD-5579 in a Principal Component Analysis. Although previous work recognized some features present on dromaeosaurid teeth, such as the serrated distal carina (Marmi et al., 2016), other characteristics (e.g., the presence of an unserrated mesial carina, large and low number of hook-shaped denticles) do not fit with that previous assignment.

Regarding the troodontid tooth MCD-5579, its overall morphology is similar to the AMNH 21874, which belongs to *Pectinodon bakkeri* from the Lance Formation of Wyoming (USA; Longrich, 2008. Fig. 9B), which was considered as a posterior dentary tooth. Both have a ziphodont, distally curved crown, and hooked denticles only on the distal carina. Denticle density for *P. bakkeri* (DAVG estimated at 3.8 denticles/mm) is just slightly higher than MCD-5579 (which ranges between 3 and 3.5 denticles/mm depending on the crown's height). The *P. bakkeri* tooth seems to be more labiolingually compressed than MCD-5579 and apparently develops transverse undulations at the middle and apical denticle height (Fig. 9B), which differs from the Molí del Baró-1 specimen.

MCD-5579 slightly resembles the premaxillary teeth of the dromaeosaurid *Saurornitholestes langstoni* from the Campanian Dinosaur Park Formation of Alberta, Canada (Currie and Evans, 2020). Both teeth share small ziphodont crowns, with a distal carina bearing relatively large denticles (although those in the Canadian specimen are more numerous and proportionally smaller; Fig. 9A, C); however, the premaxillary teeth of *S. langstoni* have a serrated mesial carina, a distal carina that is barely curved distally, bear several longitudinal flutes, and are much more compressed labiolingually. According to characters listed in Hendrickx et al. (2019), some features of MCD-5579, such as the shape and number of the denticles (hook-shaped denticles with a density less than 15 per 5 mm), rule out a dromaeosaurid affinity. TMP 82.19.180, a *Saurornitholestes* specimen from the Judith River Formation (Canada; Currie et al., 1990) that preserved several teeth, shares some similarities with MCD-5579 (Fig. 9D). In both cases, the teeth have a distally curved morphology with large denticles on the distal carina (although in MCD-5579 they are larger and seem to have more pronounced interdenticular sulci). However, TMP 82.19.180 differs from MCD-5579 in having a serrated mesial carina with denticles near the crown apex.

Furthermore, Currie et al. (1990) described numerous troodontid teeth attributed to *Troodon formosus*, most of which have a ziphodont or folidont shape (*sensu* Hendrickx et al., 2015), and both carinae with denticles (the hooked shape of the MCD-5579 denticles is less pronounced than generally recorded in *Troodon formosus* teeth). In particular, the specimen TMP 83.12.11 (Fig. 9E) lacks a mesial carina, and the shape of the distal denticles is also similar to MCD-5579. However, their main difference is the size of the denticles, with TMP 83.12.11 having mesiodistally larger denticles than MCD-5579. Sankey et al. (2002) described a tooth of *Troodon* sp. (RTMP 86.177.8) from the late Campanian Judith River Group, Alberta (Fig. 9F), which shares with MCD-5579 the ziphodont condition, the general shape in lateral views, and the large size and shape of the hooked denticles. Contrary to MCD-5579, RTMP 86.177.8 has an unserrated mesial carina with a mesial

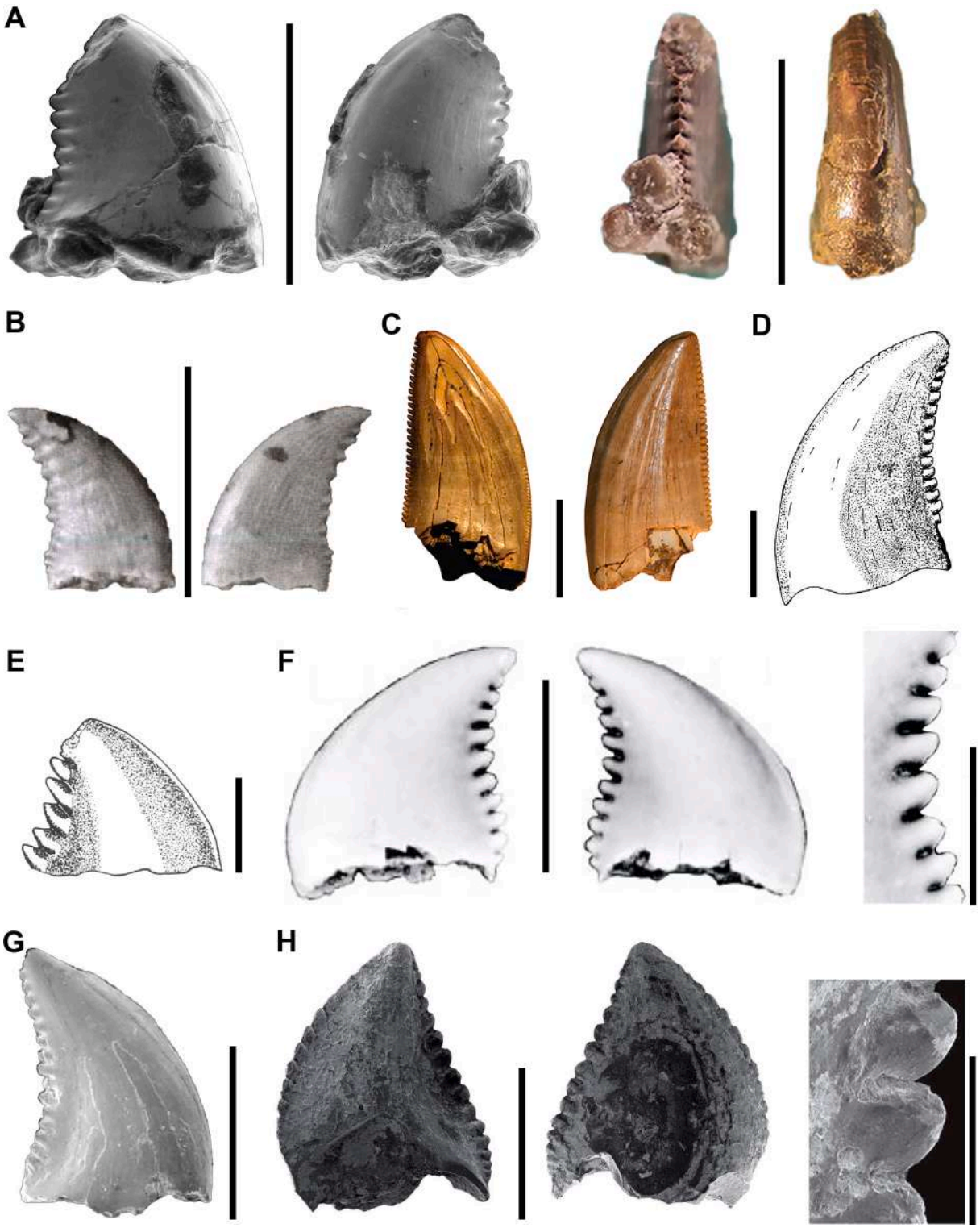

Fig. 9. Morphological comparison of MCD-5579 (Troodontidae) tooth and similar teeth. A, MCD-5579 (from left to right: lingual and labial views on SEM images, distal and mesial views on normal light); B, AMNH 21874 (*Pectinodon bakkeri*) posterior dentary tooth in lingual and labial views (extracted and modified from Longrich, 2008); C, TMP 1987.050.0008 (*Saurornitholestes*) tooth in lingual, labial, distal and mesial views (extracted and modified from Currie and Evans, 2020); D, TMP 82.19.180 (*Saurornitholestes langstoni*) tooth in lingual view (extracted and modified from Currie et al., 1990); E, TMP 83.12.11 ("*Troodon formosus*") tooth crown in lingual view (extracted and modified from Currie et al., 1990); F, RTMP 86.177.8 ("*Troodon*" sp.) tooth crown in lateral views, and detail of the distal carina denticles (extracted and modified from Sankey et al., 2002); G, indeterminate velociraptorine tooth crown in lateral view (extracted and modified from Codrea et al., 2002); H, DUGF/52 (troodontid) tooth in lingual, labial, and detail of the distal carina denticles (extracted and modified from Goswami et al., 2013). Scale bars equal 5 mm in A, B, C, D, E, 2 mm in F and G, and 1 mm for denticles detail in E, and 500 μm for denticles detail in G.

expansion at the base of the crown (Fig. 9F), which apically changes towards a carina with poorly developed denticles. Also, RTMP 86.177.8 has wider interdenticular spaces than MCD-5579. In cross-section, RTMP 86.177.8 is slightly more laterally compressed than MCD-5579 and has a lanceolate shape.

Additionally, MCD-5579 shares some similarities with a tooth assigned to Velociraptorinae from the Maastrichtian "Totesti-baraj" locality, Haţeg Basin, Romania (Codrea et al., 2002). They share a similar distally curved morphology and relatively large denticles on the distal carina (Fig. 9G). However, the Romanian tooth has a mesial carina with denticles in its apical region, smaller denticles (DAVG estimated at 6.3 denticles/mm), lacks well-developed hook-shape denticles, and the interdenticular sulci are less pronounced. Finally, it is also interesting to compare MCD-5579 with an upper Maastrichtian troodontid tooth from India (DUGF/52) described by Goswami et al. (2013) (Fig. 9H). DUGF/52 shows a lanceolate shape and is highly labiolingually compressed (especially on the lingual surface), differing from the Molí del Baró-1 tooth. As a consequence, the distal carina is much less concave than in MCD-5579 (Fig. 9A). Regarding the denticles, those at the distal carina mid-height of DUGF/52 reach a maximum of 0.25 mm of apicobasal length (DDL), which is smaller than MCD-5579 (0.33 mm). Additionally, the Indian tooth has a serrated mesial carina, with parallelogram-shaped denticles present all along the carina except near the base.

3.2. Cladistic analysis

The phylogenetic analysis produces 8099 most parsimonious trees with a Consistency Index (CI) and Retention Index (RI) of 0.211 and 0.606, respectively. These are summarized in a relatively well-resolved strict consensus tree view (Fig. 10). As acknowledged by the authors of the original dentition-based datasets, these are heuristic tools meant to help identify isolated teeth rather than a means to infer an accurate phylogeny of all theropods (i.e. Hwang, 2005; Zanno and Makovicky, 2011; Hendrickx et al., 2019). With that in mind, we note that our results incorrectly do not recover some well-known groups of theropods, but this does not hinder the use of these analyses for providing a line of evidence to help identify the Molí del Baró-1 specimens. Indeed, these teeth are recovered in different clades of non-avian theropods (Fig. 10), largely corroborating our identifications based on diagnostic characters.

MCD-5033 and MCD-5583: These teeth are recovered as sister taxa of *Velociraptor* (Fig. 10). So, the analysis grouped these velociraptorines (*Velociraptor* and MCD-5033) along with dromaeosaurids (*Tsaagan* and MCD-5583). Strikingly, these taxa being branched with the basal theropod *Daeomonosaurus*, the noasaurid *Noasaurus*, and spinosaurids (Fig. 10). Regardless, the placement of MCD-5033 as a close *Velociraptor* relative corroborates our identification of it as a velociraptorine, and the position of MCD-5583 among other dromaeosaurids supports its assignation to this family.

MCD-5582: This tooth is recovered in the strict-consensus tree within a clade that contains the tyrannosauroid *Dilong*, the basal neocoelurosaur *Ornitholestes*, and the noasaurid abelisauroid *Masiakasaurus* (Fig. 10). In this branch, MCD-5582 is established as the sister taxa of *Masiakasaurus*. Despite that MCD-5582 shares dental features with known dentated noasaurids (such as *Masiakasaurus*), other features rule out the assignment to this clade. These contrasting features are: the presence of mesial denticles reaching the cervix, the lateral displacement of the distal carina (strongly deflected labially in *Masiakasaurus* whereas in MCD-5582 it is slightly lingually displaced), the development of hooked denticles, the transverse undulations, and the presence of marginal undulations. The placement of this tooth (which we have classified as an indeterminate dromaeosaurid with microraptorine affinities) in this artificial group seems misleading and we do not consider it an accurate reflection of its affinities.

MCD-5579: The analysis placed this tooth within a small group with the troodontid *Zanabazar*, the last forming a sister taxa with *Troodon* (Fig. 10). However, other troodontids (*Byronosaurus*, *Sinusonasus*, *Almas*, and MPC D100 1128 *sensu* Hendrickx et al., 2019) are separated from mentioned taxa and form another group. Regardless, the position of MCD-5579 close to representative troodontids supports our identification of it as a troodontid based on diagnostic features.

3.3. Statistical analysis

The three main Principal Components explain nearly all the variance. PC1 explains 51.807 %, followed by the PC2 and PC3 explaining 29.594 % and 17.913 %, respectively. The eigenvalues of those Principal Components are 0.610, 0.348, and 0.211, respectively.

MCD-5033: PCA analysis (Fig. 11) shows that in PC1-PC2 and PC1-PC3 plots MCD-5033 falls within the *Richardoestesia* morphospace and just outside but relatively close to the *Velociraptor mongoliensis* morphospace, which also overlaps the *Richardoestesia* area. However, on the PC2-PC3 plot, MCD-5033 is situated inside the *Velociraptor* morphospace. As Larson (2008) noted, Velociraptorinae and cf. *Richardoestesia* morphospaces are known to overlap when dental data are subjected to multivariate analysis, suggesting that Velociraptorinae diversity is higher than indicated just by tooth morphology.

Although Marmi et al. (2016) suggested a *Richardoestesia* affinity for MCD-5033, it was based on its relatively small size and additional unspecific similarities with other teeth assigned to this genus (i.e., Currie et al., 1990; Prieto-Márquez et al., 2000; Sankey et al., 2002; Torices et al., 2015) instead of particular traits. However, the current results indicate that MCD-5033 can be reassigned to Velociraptorinae due to displaying characteristics of this maniraptorans clade, and also by having key differences with *Richardoestesia* teeth. PCA analysis (Fig. 11) recovered MCD-5033 within the *Richardoestesia* range (and being within the *Velociraptor* morphospace occasionally).

MCD-5582: MCD-5582 is recovered in the PCA analysis in a morphospace closely situated to *Troodon*, *Dromaeosaurus*, and *Saurornitholestes* (Fig. 11). In the PC1-PC2 and PC1-PC3 plots, MCD-5582 is close but outside of the *Troodon* morphospace and relatively close to the MCD-5583 tooth. However, when looking at the last two components (PC2-PC3), MCD-5582 is found within the morphospaces of *Troodon* and *Dromaeosaurus* and close to MCD-5583. Additionally, MCD-5582 is more closely situated (despite still being outside) *Saurornitholestes* morphospace than in the PC1-PC2 and PC1-PC3 plots. All these data suggest that MCD-5582 has strong affinities with Dromaeosauridae, which reinforces the assignment of this tooth to this group.

MCD-5583: Finally, the PCA analysis (Fig. 11) shows that MCD-5583 is situated very close to the *Dromaeosaurus* morphospace (but within the *Troodon* morphospace) in the plot of the first two components (PC1-PC2). On the other hand, MCD-5583 is recovered within the *Dromaeosaurus* morphospace in the plots of the components PC1-PC3 and PC2-PC3 (Fig. 11). This quantitative approach supports a new assignment to Dromaeosaurinae, although minor differences might indicate that MCD-5583 could be a different species than *D. albertensis*.

3.4. Microwear analysis

The Molí del Baró-1 theropod teeth show a clear predominance of scratches over pits, which is in concordance with the

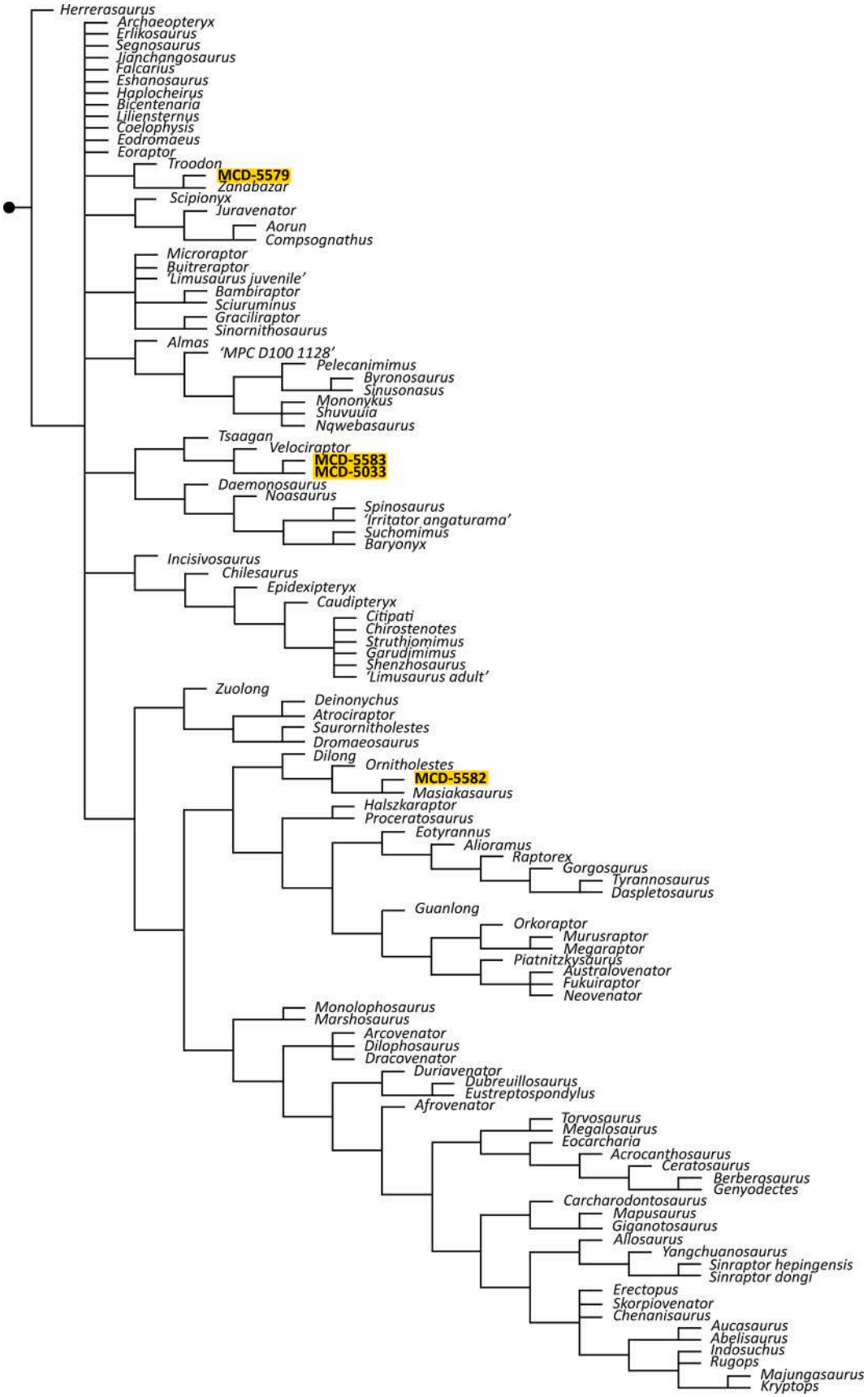

Fig. 10. Strict view cladogram showing the phylogenetic relationships of the four analysed Molí del Baró-1 theropod teeth within the theropod lineage, and the percentage of times the branches are recovered. It recovered the 8099 MPT's, resulting in a CI = 0.211, and a RI = 0.606.

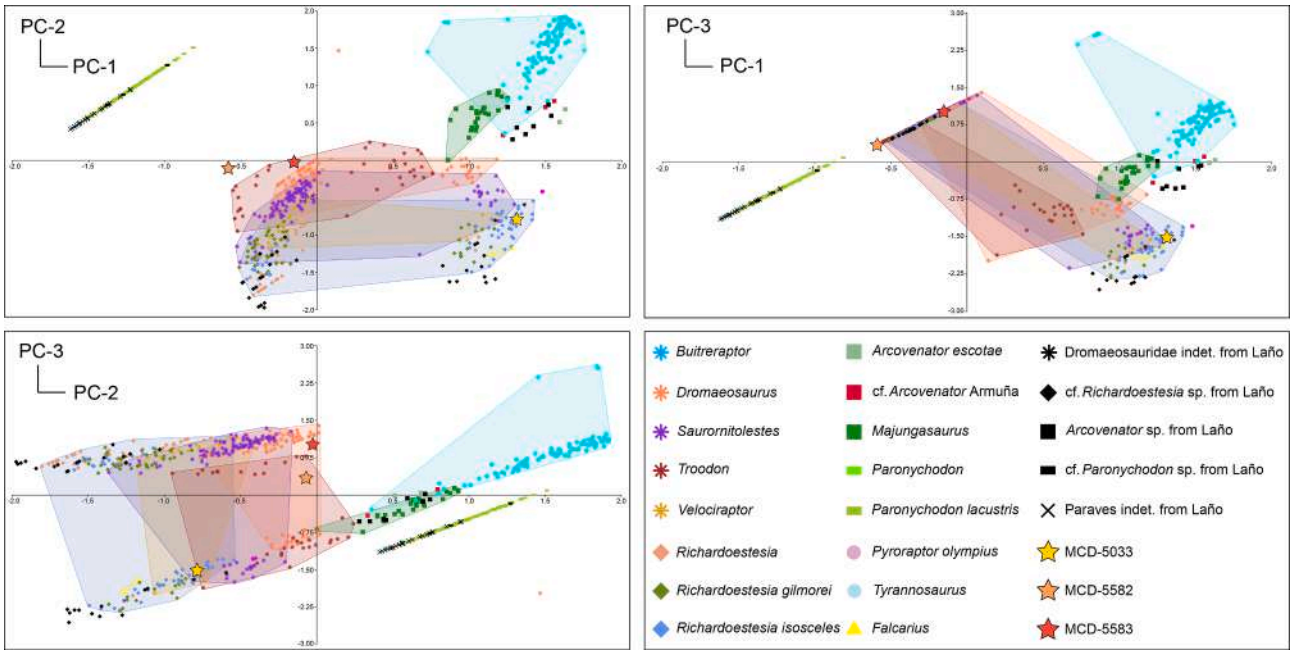

Fig. 11. PCA results with Eigenvalue values representing the variation of the taxa among the three main components. Morphospace polygons represent taxa with the same colour.

observations of previous studies (Fiorillo, 2008; Torices et al., 2018). In general, teeth preserve the two microwear-oriented families of scratches already described by Torices et al. (2018): the parallel to subparallel (considering the longitudinal plane of the crown) and the oblique families. However, a third family of perpendicular to sub-perpendicular scratches (perpendicular to the longitudinal plane of the crown) is recognized in the Molí del Baró-1 sample. In this newly recognized family, scratches and pits are preserved on both labial and lingual surfaces with very similar microwear patterns.

3.4.1. MCD-5033

This tooth records scratches and pits (Fig. 12), being dominated by scratches corresponding to the parallel family on both lingual and labial surfaces (see complete description in Supplementary Material). The second most abundant family of scratches is the oblique one, followed by the perpendicular family. Whereas scratches are present on both denticles and tooth margins, pits are restricted to the tooth margins. Additionally, MCD-5033 does not show wear facets (Fig. 12). Scratches belonging to the parallel-to-subparallel family project rectilinear traces of varying lengths (Table 1). Scratches belonging to the perpendicular family run perpendicular to the crown's longitudinal plane (Fig. 12A-C). The crown apex shows different scratch patterns between the lingual and labial surfaces: the lingual one contains a greater number of scratches of all the three families and pits compared to the abundance recorded on the labial surface. Along the crown, the parallel to subparallel scratches often display crossing structures with the oblique and perpendicular families of scratches. Oblique scratches are arranged in two different populations along the crown: those tilting towards the mesial carina (among 7° to 34°) and those tilting distally (ranging between 7° to 67°; Fig. 12C-E, Table 1). This family of scratches can display a projection of rectilinear or curved scratches. The perpendicular family of scratches can also develop rectilinear or curved structures, but with a slope between 57° and 76° (Table 1) relative to the long axis of the crown. It is noteworthy to mention that this last family of scratches sometimes has wider scratches than the other families on this tooth, reaching values of 3–6 μm and up to 8 μm in width. Finally, pits have subcircular to oval outlines (being between 8 μm and 16 μm in diameter), showing rounded and irregular margins (Fig. 12C).

3.4.2. MCD-5579

This tooth only displays a serrated distal carina, showing abundant scratches along the denticles and the crown's surfaces and even pits (Fig. 13). However, it lacks wear facets. On MCD-5579, the main family of scratches is represented by the perpendicular family, followed by the oblique family, and lastly by the parallel family. All of them are also present in the mesial margin (where they develop long scratches; Fig. 13D, Table 1). Parallel scratches are rectilinear and are overall proportionally shorter than those of the other families. Within the oblique family, the morphology of their scratches is sub-straight or curved. Also, mesially tilting scratches (14° to 68°) are more abundant than the distally tilting ones (35° to 84°; Fig. 13C-G, Table 1). The perpendicular family of scratches includes both curved and straight scratches, whose tilt ranges from 51° to 98° (Table 1). It is noteworthy to mention the differences among the lingual and labial surfaces of a well-preserved and complete denticle (Fig. 13E and F); the lingual surface shows a greater number of scratches and a smoother enamel texture than the labial surface. When looking in detail at the mesial margin, the oblique family of scratches is the most abundant (Fig. 13D), followed by the parallel to subparallel family. Crossing structures are abundant on this tooth, on all its surfaces and margins, generally being produced by the perpendicular and the oblique scratches (Fig. 13C-G). Pits have a circular to subcircular shape (ranging between 10 and 23 μm in diameter; Table 1) and are mostly restricted to the labial surface.

3.4.3. MCD-5582

Despite being damaged, this tooth still preserves scratches, which are relatively scarce and situated near the carinae of both lingual and labial surfaces (Fig. 14A-L). The parallel to subparallel family of scratches is most common, followed by the oblique and perpendicular families, respectively. On the labial

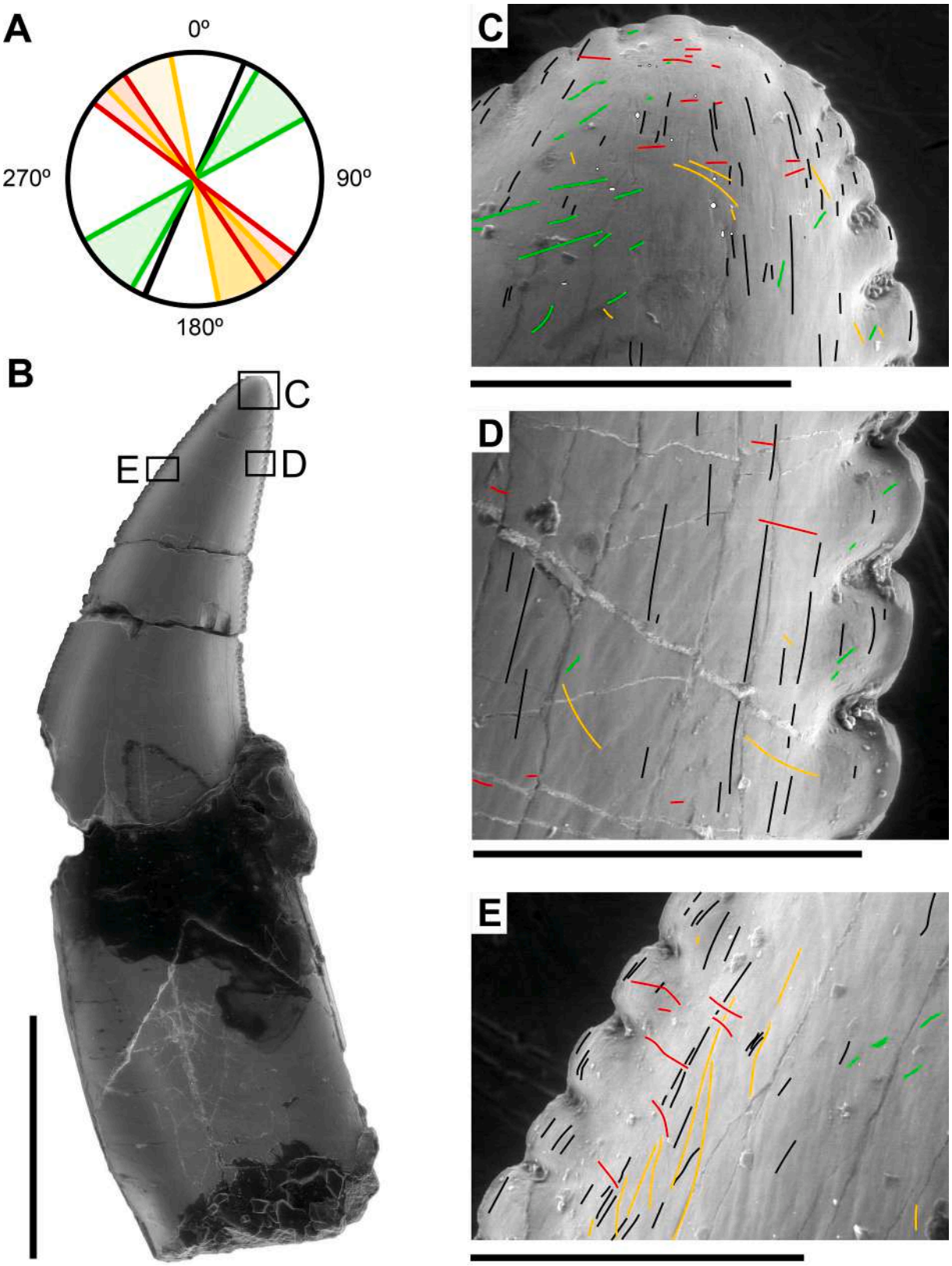

Fig. 12. MCD-5033 (Velociraptorinae) microwear results. A, microwear scratches orientations of the distal carina; B, general lingual view in SEM, with indication of selected close-up images depicting scratches families; C, close-up of the crown apex; D, close-up of the distal carina; E, close-up of the mesial carina caption. Colour legend: Crown long axis and the parallel to subparallel scratches in black; mesially tilting oblique scratches in green, distally tilting oblique scratches in orange, and perpendicular to sub-perpendicular scratches in red. Scale bars equal 5 mm in A, and 500 μm in C, D, and E.

Table 1
Microwear measurements of the Molí del Baró-1 theropod teeth, divided into distal and mesial carinae, and inside of each the scratches length and sloping angle (this last regarding the longitudinal plane of the crown). All measurements in micrometres (μm). Abbreviations: dc, distal carina; mc, mesial carina; scr, scratches.

	MCD-5033	MCD-5579	MCD-5582	MCD-5583
dc. parallel scr. length	14–60 (100–186) μm	90–120 μm	20–290 μm	20–464 μm
dc. oblique scr. (mesial) length	30–34 μm	80–300 μm	20–360 μm	25–467 μm
dc. oblique scr. (distal) length	19–53 μm	30–100 μm	20–220 μm	25–467 μm
dc. perpendicular scr. length	46–108 μm	15–420 μm	20–156 μm	30–196 μm
dc. oblique scr. (mesial) angle	7–32°	14–68°	14–28°	12–52°
dc. oblique scr. (distal) angle	34–67°	35–84°	13–66°	8–66°
dc. perpendicular scr. angle	57–76°	51–96°	53–102°	63–137°
mc. parallel scr. length	17–75 μm	300–550 μm	25–300 μm	40–780 μm
mc. oblique scr. (mesial) length	20–90 μm	134–511 μm	32–145 μm	56–550 μm
mc. oblique scr. (distal) length	32–304 μm	120–544 μm	10–160 μm	25–220 μm
mc. perpendicular scr. length	31–85 μm	22–590 μm	9–210 μm	58–160 μm
mc. oblique scr. (mesial) angle	22–34°	33–63°	20–44°	29–59°
mc. oblique scr. (distal) angle	7–47°	36–62°	7–50°	6–26°
mc. perpendicular scr. angle	55–74°	73–98°	85–114°	87–114°
Scratches mean width	0.8–1.2	2; 0.8–1.1	1.2	1.5–2.1
Pitting (outline diameter)	1.4–3.8; 8–16 μm	10–23 μm	10–20 μm	7–32 μm

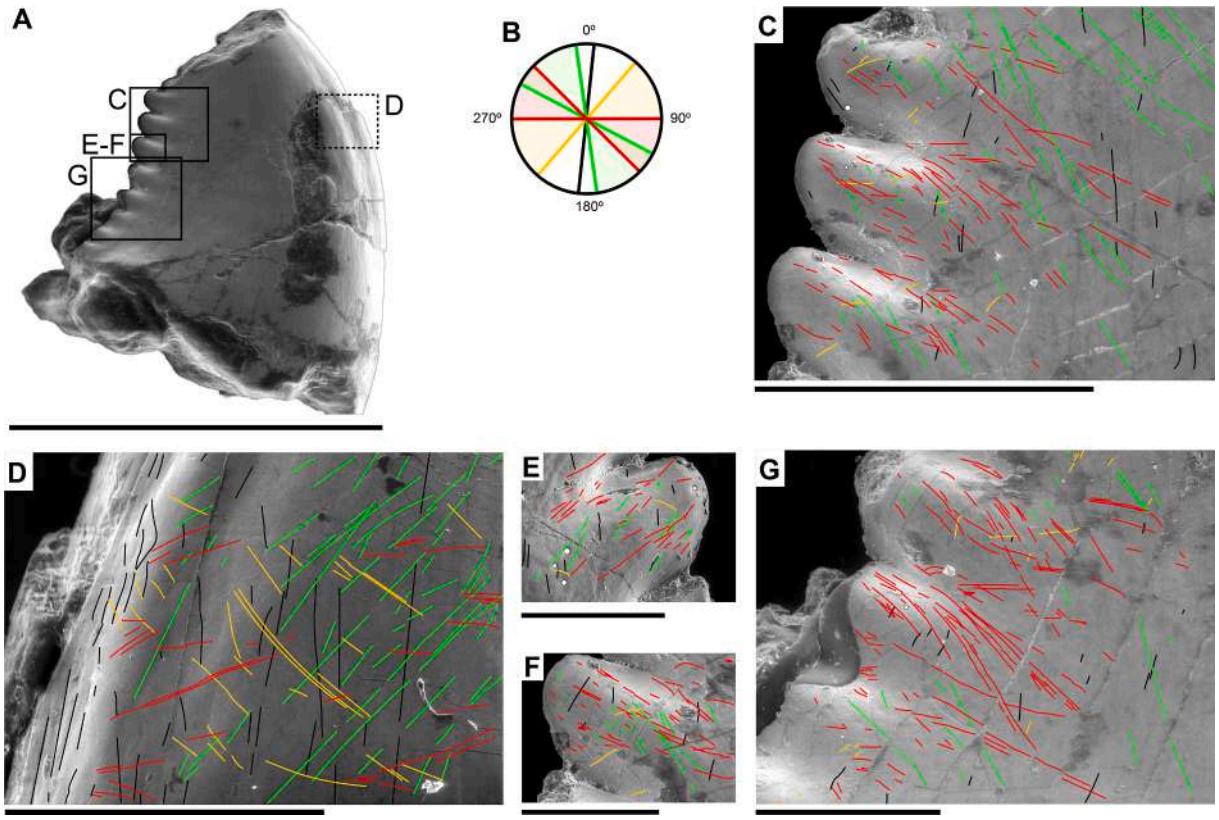

Fig. 13. MCD-5579 (Troodontidae) microwear results. A, general SEM view of the tooth in lingual view and the selected close-up views; B, microwear scratches orientations of the distal carina; C, close-up SEM view of the mid-height to apical denticles in the distal carina; D, close-up SEM view of the mesial carina in labial view; E, close-up SEM view of the distal carina caption in labial view; F, close-up SEM view of the distal carina caption in lingual view; G, close-up SEM view of the basal distal carina with denticles. Colour legend: crown long axis and the parallel to subparallel scratches in black, mesially tilting oblique scratches in green, distally tilting oblique scratches in orange, and perpendicular to sub-perpendicular scratches in red. Dashed line in A indicates that the caption is from the labial margin. Scale bars equal 5 mm in A, 1 mm in C and D, and 400 μm in E and F, 500 μm in G.

surface, scratches are significantly more abundant than on the lingual surface (note the different number of scratches in Fig. 14D-L). The tooth lacks wear facets but has several crossing structures and a few pits. Notably, the tilting range of scratches for each family is well differentiated in this tooth (Table 1). Scratches from the parallel family generally display a rectilinear morphology but they show different lengths. As observed in the previous teeth, the family of oblique scratches is divided in two populations, having a close proportion between these two and developing relatively low angles, with over 22° and 37° for the mesial and distally tilting populations, respectively (Fig. 14B, Table 1). Scratches from the mesial population predominantly display straight shapes, whereas the distal population generally develops curved projections (e.g., Fig. 14D-F, I-L). For the family of perpendicular to sub-perpendicular scratches, their structures are typically rectilinear and have a tilting range between 53° and 114° (Table 1) relative to the crown's elongated plane (Fig. 14B, D, H, I-L). Pits are scarce in this tooth. They have a subcircular shape with a diameter between 10 and 20 μm (Fig. 14E, G).

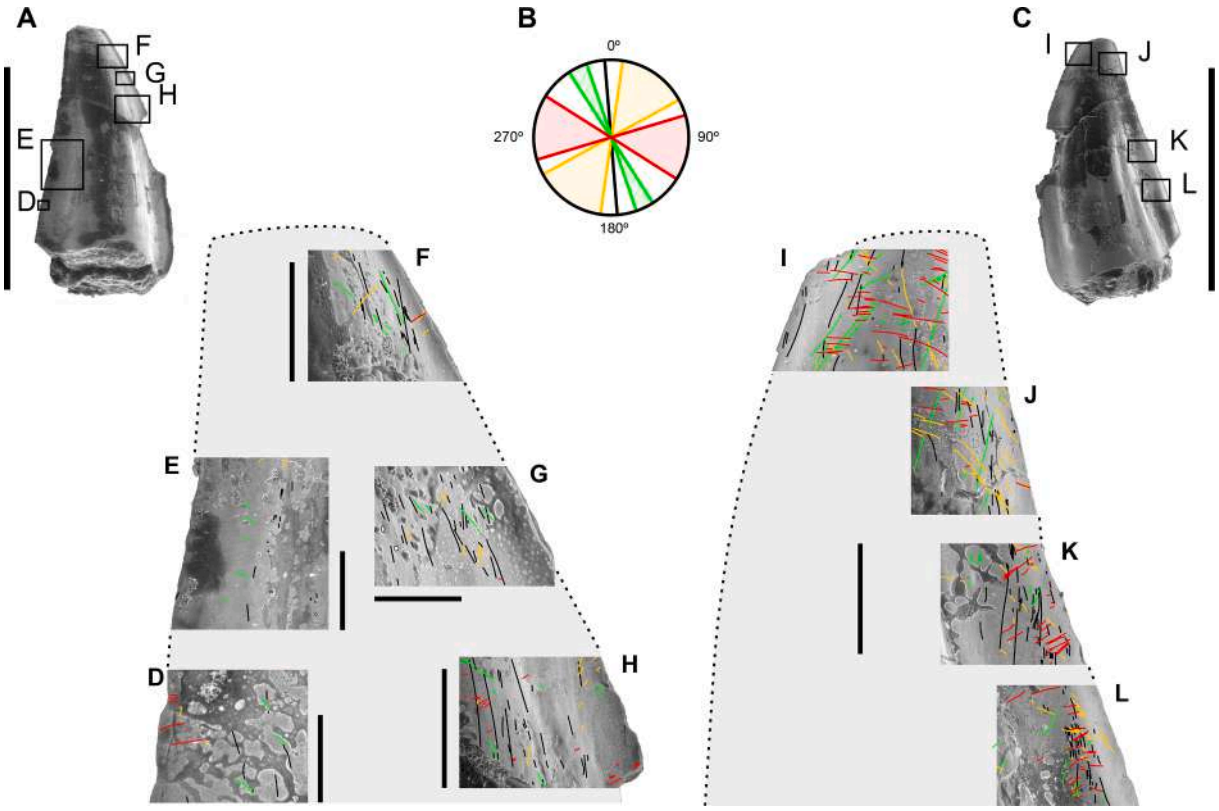

Fig. 14. MCD-5582 (Dromaeosauridae indet.) microwear results. A, general views of the tooth in lingual view and the selected close-up views; B, microwear scratches orientations of the distal carina; C; general views of the tooth in labial view and the selected close-up views; D and E, close-up SEM images of the distal carina in lingual view where it is possible to recognize the denticles; F to H, close-up SEM images of the mesial carina in lingual view at different heights; I, close-up SEM image of the apical mesial carina in labial view; J-L, close-up SEM images of the distal carina in labial view at different heights. Colour legend: crown long axis and the parallel to subparallel scratches in black, mesially tilting oblique scratches in green, distally tilting oblique scratches in orange, and perpendicular to sub-perpendicular scratches in red. Scale bars equal 5 mm in A and C, 500 μm in E, F, H, I to L, and 200 μm in D and G.

3.4.4. MCD-5583

The tooth has abundant scratches on the mesial and distal margins and few in on the distal carina (Fig. 15A-E). Pits are also recorded. In the apical region, there are 2 two wear facets (Figs. 15 and 16), and all along the crown there are numerous crossing structures (Fig. 15C-E). Generally, parallel to subparallel and oblique scratch families have the same overall predominance in terms of abundance, whereas the perpendicular to subperpendicular family is the scarcest. However, in the mesial carina there is a predominant family of scratches represented by parallel to subparallel structures (Figs. 15 and 16B-E). Generally, parallel scratches have a straight morphology, as do the oblique scratches. However, the latter family can also exhibit curved shapes more often than the parallel family (Fig. 15C-E). The mesially tilting population of oblique scratches is more abundant than the distal population, tilting between 12 and 59° and 6 to 66° respectively (Fig. 15A; Table 1). The perpendicular scratches can display both curved and rectilinear morphologies (Fig. 15C-E) and a tilt restricted between 87 and 114° (Table 1). Regarding the presence of pits, they are frequent and can be found all over the crown (Figs. 15C-E and 16B-D) with a circular or irregular outline (between 7 and 32 μm; Table 1).

4. Discussion

4.1. Palaeoecological inferences

Tooth microwear analyses have been used to infer diets and chewing patterns among theropods (i.e., Torices et al., 2018; Winkler et al., 2022). When applied to teeth from the Molí del Baró-1 locality, similar analyses reveal a variety of microwear patterns among the theropod teeth assemblage (Fig. 17), possibly implying different feeding roles among the small theropods during the uppermost Maastrichtian.

MCD-5033 (Figs. 12, 17) is characterized by a predominant family of parallel to subparallel scratches, followed by a set of oblique ones, which are similar to observed on *Gorgosaurus* and cf. *Pyroraptor* (Torices et al., 2018). Perpendicular scratches are less abundant. This suggests that these scratches might have been produced through a 'puncture-and-pull' feeding mechanism, a feeding behaviour that has been inferred for dromaeosaurids (Torices et al., 2018).

Among the Molí del Baró-1 sample, the troodontid tooth MCD-5579 has the most abundant and prominent perpendicular to subperpendicular scratches (Figs. 13, 17). The parallel to subparallel scratches are less abundant on the distal carina but more frequent on the mesial margin. This pattern of scratches suggests that this tooth probably did not perform the typical 'puncture and pull' mechanism but a more specific and/or specialized one. For instance, the relatively low number of parallel scratches might imply that the food source was softer and/or smaller than that inferred for MCD-5033 (Fig. 17). However, the 'pull' component was undoubtedly present, producing the numerous mesial oblique scratches distributed along the whole crown.

The microwear pattern observed on MCD-5579 resembles, in some aspects, that observed in some *Troodon* teeth (Torices et al., 2018). Moreover, the perpendicular scratches in MCD-5579 (Figs. 13, 17) are straight (or very slightly curved), suggesting that

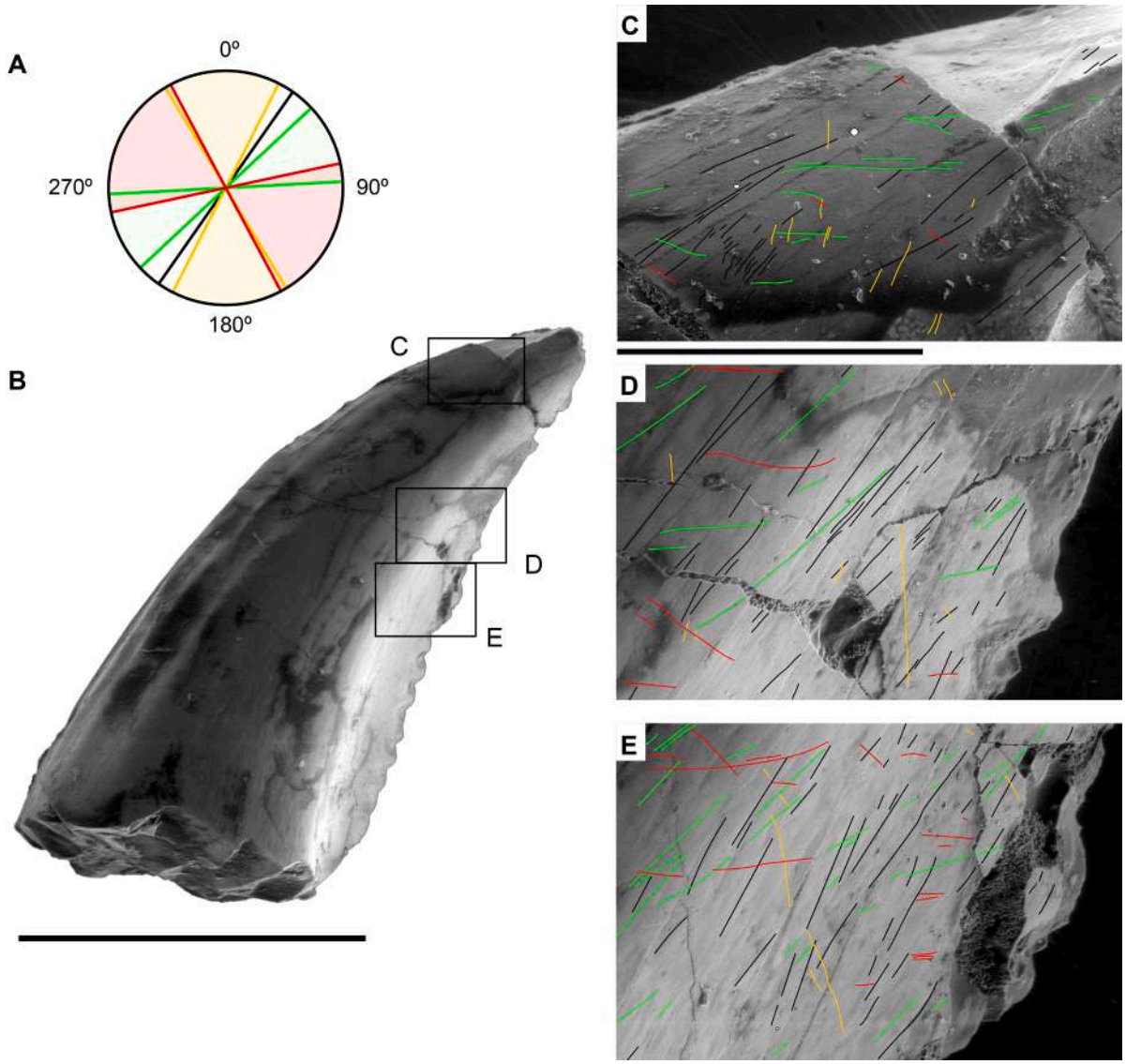

Fig. 15. MCD-5583 (Dromaeosaurinae) microwear results. A, microwear scratches orientations of the distal carina; B, microwear scratches orientations of the distal carina and general SEM image of the tooth in lingual view, with indication of the close-up captions; C, close-up SEM image of the mesial margin in lingual view; D, close-up SEM image of the mid-apical distal carina in lingual view; E, close-up SEM image of the mid height distal carina in lingual view. Colour legend: crown long axis and the parallel to subparallel scratches in black, mesially tilting oblique scratches in green, distally tilting oblique scratches in orange, and perpendicular to sub-perpendicular scratches in red. Scale bars equal 5 mm in B, 1 mm in C, D, E.

they were produced as a response to a sustained "grip" of the flesh or food source (or alternatively, a "pulling back and tugging" movement produced when feeding on carcasses; Wings et al., 2015), without any vertical movement. Therefore, the "puncture and pull" system would not be the main feeding mechanism for the individual that lost this tooth, as previously proposed for troodontids and therizinosauroids (Holtz et al., 1998). If so, these scratches could have been produced passively by the prey movements when it was still grabbed, instead of an active movement of the predator (Wings et al., 2015). Grabbing the prey with the mouth might have been a strategy to reduce the prey's movements or produce injuries in vital points (such as the neck).

Alternatively or additionally to this, the microwear pattern might have been produced by a movement of pulling back the flesh without the need of puncturing (i.e., in a comb or rake-like movement), which subsequently makes possible inferring a substantial degree of plant content in their diet. A phytophagous diet was previously proposed for theropods through different approaches, including for troodontids (Holtz et al., 1998; Zanno et al., 2009; Lü et al., 2010; Zanno and Makovicky, 2011; Larson et al., 2016; Cullen and Cousens, 2023). Cullen and Cousens (2023) used isotopic geochemical analyses to demonstrate a plant-dominant omnivorous diet for troodontids, incorporating other dietary components, such as small to medium vertebrates.

We interpret the scratch pattern of MCD-5579 as reinforcing the idea of an omnivorous diet, with a predominance of plants, for troodontids. A mainly phytophagous dietary content is supported by the low number of parallel scratches (that would not likely be produced in the situation of reaching a leaf or branch and subsequently plucking it) and by the significant accumulation of perpendicular scratches on the interdenticular sulci. These latter scratches could have been caused by the concentration of leaf veins and small branches passing through interdenticular sulci,

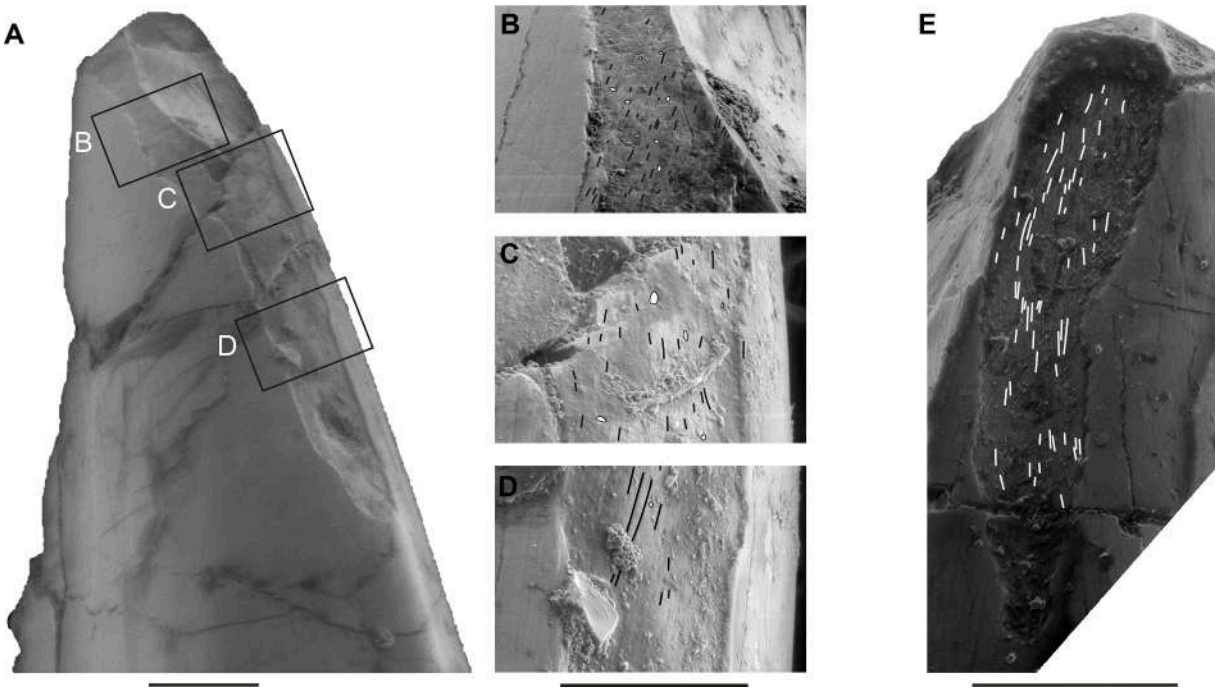

Fig. 16. MCD-5583 (Dromaeosaurinae) microwear results. A, general SEM image of the tooth in mesio-labial view with indication of selected caption; B, C, and D, close-up SEM images of the mesial carina at different heights; E, close-up SEM image of the lingual surface. Scale bars equal 1 mm in A, and 500 μm in B to E.

with the large-sized denticles developing a comb-like structure. This proposal concurs with the results of Torices et al. (2018), which indicate that troodontid denticles might have been vulnerable to breakage if high stress forces were applied at non-optimal cutting angles.

Another supporting point for plant-heavy omnivorous diet in troodontids are traits in basal troodontids (such as *Jinfengopteryx*) that correlate with herbivorous feeding (Zanno and Makovicky, 2011). The lack of a lanceolate crown shape, a characteristic seen in derived troodontids, suggests that MCD-5579 may be related to basal troodontids. Furthermore, MCD-5579 has pits on both distal region surfaces, which suggests consumption of hard objects (such as bone fragments, hard vegetation, seeds, or insects). The consumption of hard objects is in line with the observation of an area with abundant pits over the labial cervix together with the record of wider and parallel scratches on the mesial margin (Fig. 13). Various authors (Fiorillo, 1998; Mallon and Anderson, 2014) reported populations of scratches in Late Cretaceous megaherbivores (sauropods, ankylosaurids, nodosaurids, centrosaurines, chasmosaurines, hadrosaurines, and lambeosaurines) ranging from $\leq$2 μm to 26 μm. In MCD-5579, we recorded thick scratches that range from 2 to up to 14 μm, although most of the values are between 0.8 and 1.1 μm. These values fall within the range of scratch widths observed in megaherbivores, opening the possibility supporting the hypothesis that some troodontid scratches were produced by plant components. Finally, the function of the crossing structures (Figs. 13, 17) is not clear, although they seem to follow the formation model proposed by Torices et al. (2018) and thus were related to some head movements.

In the dromaeosaurid tooth MCD-5582, parallel to subparallel scratches are the dominant family (Figs. 14, 17), and this might indicate the use of the puncture and pull feeding mechanism. However, another feeding mechanism may also be suggested for this tooth due to the presence of a significant proportion of perpendicular to sub-perpendicular scratches. Following this, as pits are not located at the carinae margins but in a more equatorial position on the lingual and labial sides, they might have been produced during the consumption of hard food (such as seeds, fruits, or even invertebrates). Further, if the affinity with microraptorines is considered, it is worth mentioning the alleged omnivorous diet, or at least not strictly carnivorous diet, of members of this clade (Li et al., 2020).

Scratches in MCD-5583 likely were produced by a typical puncture and pull mechanism (as in MCD-5033), as few perpendicular scratches are recorded, but instead a predominance of parallel and oblique scratches are present. Finally, it is worth mentioning that the tilting degree ranges of the oblique scratches on the Molí del Baró-1 teeth are similar to those observed in the sample studied by Torices et al. (2018), thus representing the general pattern expected for theropod teeth used in puncture and pull feeding mechanisms.

4.2. Theropod diversity at the Molí del Baró-1 locality

The previous study by Marmi et al. (2016) proposed the presence of several theropod taxa at the Molí del Baró-1 locality based on shed teeth. They recognized the presence of dromaeosaurids and possibly *Richardoestesia*, *Paronychodon*, and "*Euronychodon*" (*sensu* Rauhut, 2002; Torices et al., 2015), along with other indeterminate forms. Our review of these specimens supports the presence and a notable abundance of small-sized maniraptoran taxa at the locality, including indeterminate dromaeosaurids (likely microraptorines), dromaeosaurines, velociraptorines, troodontids, cf. ?*Richardoestesia* and aff. *Paronychodon*, highlighting a diverse faunal assemblage in the uppermost Maastrichtian (C29r) on the Ibero-Armorican island. This concurs with the high theropod diversity recorded by Isasmendi et al. (2024) for the upper Maastrichtian of the western Pyrenees.

Dromaeosaurines and velociraptorines are well-documented in the Maastrichtian dinosaur assemblages of south-western Europe

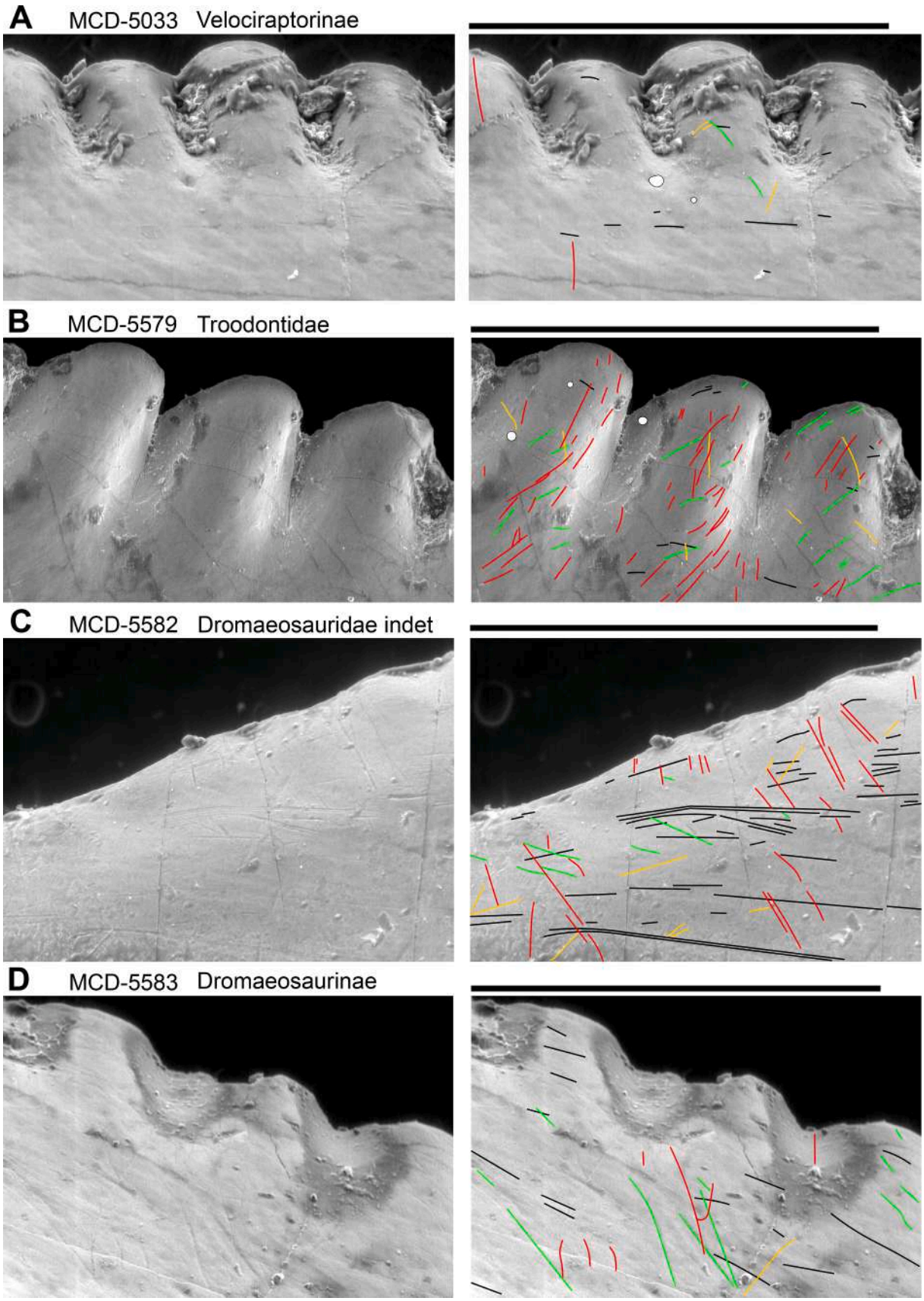

Fig. 17. Microwear on the Molí del Baró-1 theropod sample. Left column, unmodified SEM images; right column, scratches and pitting structures coloured (black: parallel to subparallel and crown's longitudinal plane; mesial oblique: green; distally oblique: yellow; perpendicular to sub-perpendicular: red). Scale bars equal 500 μm in A and C, and 1 mm in B and D.

(Csiki-Sava et al., 2016; Isasmendi et al., 2022, 2024; Malafaia et al., 2023). As for Troodontidae, the assignment of MCD-5579 to this family supports the presence of the clade in the latest times of the Maastrichtian in the Ibero-Armorican island. Interestingly, the presence of an indeterminate dromaeosaurid (MCD-5582) with remarkable similarities with microraptorines is striking because indisputable remains of this clade are nearly exclusive from the Lower Cretaceous of Liaoning, China (Maranga, 2021 and references therein), and probably from the Upper Cretaceous of North America (Longrich and Currie, 2009). One exception is the younger partial skeleton of *Hesperonychus* from the Dinosaur Park Formation, Alberta, Canada (Longrich and Currie, 2009), which potentially extends the record of the clade around 45 My, from middle Aptian to upper Campanian, although we note that large-scale phylogenetic analyses have sometimes found this species to be a wildcard taxon that is not clearly recovered as a microraptorine (e.g., Brusatte et al., 2013). The potential presence of a microraptorine in the upper Campanian of North America led us to more strongly speculate the occurrence of this group in the uppermost Maastrichtian of Europe as well. Unfortunately, the *Hesperonychus* holotype and referred material lack teeth (Longrich and Currie, 2009), preventing a direct comparison with the Molí del Baró-1 specimen. If further studies on MCD-5582 confirm its microraptorine affinities, then this would represent the first occurrence of this clade in the Cretaceous of Europe and the youngest record worldwide. At the very least, regardless of its taxonomic placement, this tooth indicates that small paravians of similar size and ecology to microraptorines were components of the uppermost Cretaceous European faunal assemblages.

4.3. Late Maastrichtian theropod assemblages

In Europe, some authors have proposed that during the early upper Maastrichtian (C31r–C31n), ecosystems of the Ibero-Armorican island were restructured by the arrival of several dinosaur clades around 69 Ma as a result of marine regressions, favouring the introduction of new groups of iguanodontian ornithopods and titanosaurian sauropods (Le Loeuff et al., 1994; Vila et al., 2016; Fondevilla et al., 2019). This event, called the 'Maastrichtian Dinosaur turnover', produced changes in the predominance of some dinosaur clades over others, with small changes also for theropod fauna (Vila et al., 2016; Isasmendi et al., 2024). Basically, it was composed of small-sized taxa as velociraptorines, dromaeosaurines, indeterminate dromaeosaurids, *Richardoestesia*, and *Paronychodon,* alongside abelisaurids (Fig. 18). Currently recorded abelisaurids typically represent part of the pre-turnover assemblages (Vila et al., 2016), being predominantly recorded on the Ibero-Armorican island from the upper Campanian to the lower Maastrichtian (Tortosa et al., 2014; Isasmendi et al., 2022; Malafaia et al., 2025). Abelisaurids likely arrived on the Ibero-Armorican island during Gondwanan dispersal events, most probably through northern Africa (Gheerbrant and Rage, 2006; Pereda-Suberbiola, 2009; Ezcurra and Agnolín, 2012; Isasmendi et al., 2022; Longrich et al., 2023). As an effect of the Maastrichtian Dinosaur turnover, at the end of the Maastrichtian, the Ibero-Armorican island was also populated by troodontids (Sellés et al., 2021; Pérez-Pueyo et al., 2021). As a whole, the late Maastrichtian theropod assemblage on the Ibero-Armorica island differs from that observed in other contemporary regions (Fig. 18).

In the eastern part of the European archipelago, the Haţeg island also records small theropod specimens, many of which are shared with the Ibero-Armorican assemblage. These forms are: troodontids, velociraptorines, dromaeosaurines, indeterminate dromaeosaurids, *Richardoestesia*, and *Paronychodon* (Csiki-Sava et al., 2015, 2016). This island also has yielded the bizarre dromaeosaurid (or possible avialan: Cau et al., 2015) *Balaur* (Csiki et al., 2010; Brusatte et al., 2013), the alvarezsaurid *Heptasteornis* (Naish and Dyke, 2004) and the enigmatic *Elopteryx* (Kessler et al., 2005; Csiki-Sava et al., 2016, Fig. 18), whose records have not been reported yet in other islands of the European archipelago. Regarding the latter two taxa, their assignment to Alvarezsauridae is still a topic of debate (Csiki-Sava et al., 2015, and references therein), and the possibility that these two taxa were the same should not be ruled out (Le Loeuff, 1992; Csiki and Grigorescu, 1998). The main differences with the records of the Ibero-Armorican island is the absence of abelisaurids or other mid-to-large-sized theropods in the Haţeg ecosystems, and that troodontids are restricted to the interval C31n-C30n but absent in the C29r in Romania. Csiki-Sava et al. (2015) considered the European archipelago as an individual bioprovince; however, a detailed analysis suggests that probably these minor differences among islands in their non-avian theropods (but also in other groups like the lambeosaurine hadrosaurids) indicate a more complex biogeographic history for the vertebrate faunas, which may have been shaped by numerous idiosyncratic dispersal and isolation events (Weishampel et al., 2010; Pérez-Pueyo et al., 2019).

In North Africa, the theropod record in Morocco during the upper Maastrichtian is still scarce. However, this assemblage highly differs from that from the Ibero-Armorican island, since it is exclusively composed of medium-to large abelisaurids (Longrich et al., 2017, 2023) and apparently lacks the small paravian theropod forms recorded in the European archipelago (Fig. 18), although this may be a figment of sampling bias. The bias might also affect the record of small and ontogenetically earlier forms of medium and large known forms (on a global scale, not just in this region), as younger individuals necessarily have to be significatively more numerous than adults, possibly masking their abundance. In western Gondwana, the Brazilian Marília Formation (dated as upper Maastrichtian, 70.6 to 65.5 m.a.; Dias-Brito et al., 2001; Abreu Filho and Albuquerque, 2016; Brusatte et al., 2017) has yielded a relatively wide variety of non-avian theropods. As on the Ibero-Armorican island, derived maniraptorans (Novas et al., 2005) and abelisaurids (Candeiro et al., 2008; Novas et al., 2008) were present (Fig. 18). However, the Brazilian record clearly suggests a proportionally higher abundance of abelisaurids than in the Ibero-Armorican record, as the Brazilian abelisaurids include the medium-sized abelisaurid *Kurupi itaata* (Iori et al., 2021) and multiple indeterminate taxa (Candeiro et al., 2008; Novas et al., 2008). Furthermore, the Marília Formation also records the presence of the small-sized indeterminate theropod *Ypupiara lopai* (Brum et al., 2021; Motta, 2023). Geographically close by, the La Colonia Formation (Argentina) is dated also to the upper Maastrichtian (Clyde et al., 2021) and the current record is restricted to abelisaurid non-avian theropods such as *Carnotaurus sastrei* (Bonaparte, 1985) and *Koleken inakayali* (Pol et al., 2024). Still in Gondwana, the Indian subcontinent records a similar non-avian theropod assemblage to that of Morocco during the upper Maastrichtian, exclusively represented by abelisauroids such as *Rajasaurus* (Wilson et al., 2003), *Rahiolisaurus* (Novas et al., 2010), indeterminate abelisaurids (Prasad et al., 2016), and noasaurids (Mohabey et al., 2024 and references therein). Moreover, Goswami et al. (2013) reported the presence of an isolated troodontid tooth in India. Despite the presence of a troodontid, the Indian assemblage contrasts with those from the European archipelago at the end of the Maastrichtian by the absence of an abundant assemblage of small-sized maniraptorans (Fig. 18).

The China assemblage during the upper Maastrichtian also differs from the non-avian theropod fauna of the Ibero-Armorican island as it lacks any of the recognized European taxa. This

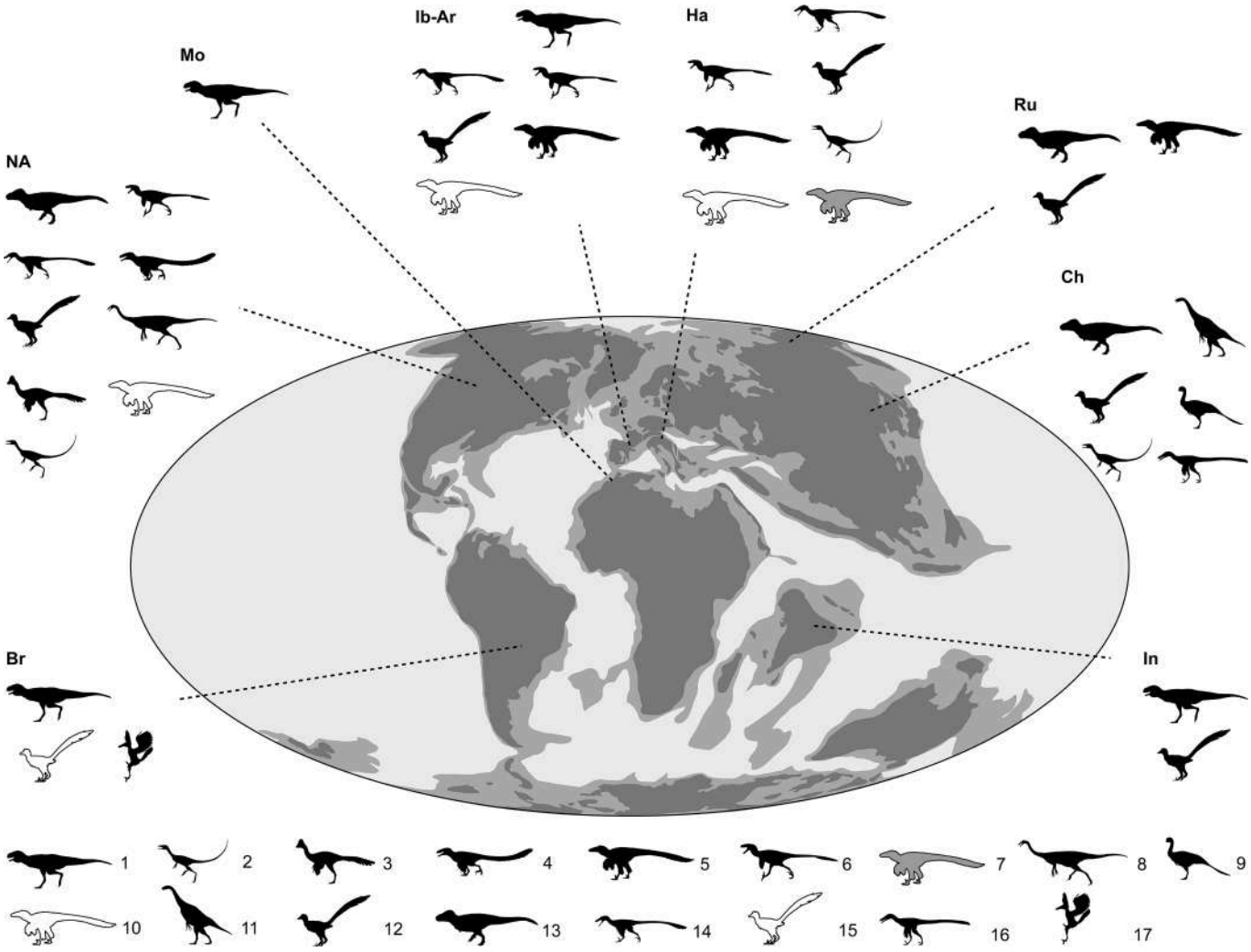

Fig. 18. Global non-avian theropod diversity in the late Maastrichtian. Color legend in A corresponds to: Sea (pale grey), Continental platform (grey), and Exposed landmass (dark grey). Abbreviations: Br: Brasil; Ch: China; Ib-Ar: Ibero-Armorican island; In: India; Ha: Hațeg island; Mo: Morocco; NA: North America; Ru: Russia. 1: Abelisauridae; 2: Alvarezsauridae; 3: Caenagnathidae; 4: large dromaeosaurid; 5: Dromaeosauridae; 6: Dromaeosaurinae; 7: *Elopteryx*; 8: Ornithomimidae; 9: Oviraptorosauria; 10: *Richardoestesia* + *Paronychodon*; 11: Therizinosauridae; 12: Troodontidae; 13: Tyrannosauridae; 14: Velociraptorinae; 15: Derived maniraptoran; 16: Small theropods; 17: *Ypupiara*. Silhouettes (not at scale) extracted and modified from PhyloPic (https://www.phylopic.org/). Palaeomap extracted and modified from Scotese (2014).

particular assemblage is represented by oviraptorosaurs, tyrannosauroids, therizinosaurids, small theropod taxa (Russell et al., 1993; Han et al., 2022), plus small alvarezsaurids (as *Qiupanykus*, Lü et al., 2018; Fig. 18). Apparently, troodontids were absent in this assemblage at the end of the Cretaceous, whereas they persisted in other regions of Asia. Conversely, the assemblage of non-avian theropods from eastern Siberia (Russia) shares a similar structure as that observed on the Ibero-Armorican island, despite being at higher latitudes (Godefroit et al., 2009). This community of theropods is represented by diverse families of small-sized theropods as dromaeosaurids and troodontids, together with large-sized forms like tyrannosauroids (Tumanova et al., 2004; Godefroit et al., 2009, Fig. 18). However, the Ibero-Armorican island shows a richer diversity of small forms, and large theropods niches were held by abelisaurids instead of tyrannosauroids.

On the Laramidia and Appalachia continental masses of present-day North America, the upper Maastrichtian theropod record is highly diverse, sharing with that of the Ibero-Armorican island multiple clades of small non-avian theropods: dromaeosaurines, velociraptorines, troodontids, *Richardoestesia*, and *Paronychodon* (Sankey, 2008; Longrich, 2008; Zelenitsky et al., 2017; Jasinski et al., 2020). However, these landmasses had their own groups of medium and large forms: caenagnathid oviraptorosaurs (Lamanna et al., 2014; Bell et al., 2015), large dromaeosaurids (DePalma et al., 2015), tyrannosaurids (Gates et al., 2013; Stein, 2019), and ornithomimids (Claessens and Loewen, 2016) (Fig. 18). Aside from that, there is the small to intermediate sized alvarezsaurid *Trierarchuncus prairiensis* (Fowler et al., 2020, Fig. 18), being this lineage absent in the Ibero-Armorican association. It is therefore remarkable that the Ibero-Armorican island lacks the medium-sized forms, which were taxonomically and ecologically diverse in North America during the late Maastrichtian, although taphonomic biases cannot be ruled out as an explanation.

4.4. Palaeobiogeography of the Ibero-Armorican troodontids

Troodontids were present nearly exclusively on the Laurasian landmasses and persisted in Europe until the end of the Maastrichtian (C29r) (Sellés et al., 2021). However, if the known fossil record is taken at face value, troodontids were apparently absent on the Ibero-Armorican island (Pérez-Pueyo et al., 2019; Isasmendi

et al., 2024) during most of the entire Maastrichtian (72–66.5 m.a.) but present during at least some of this time on the eastern Haţeg island. Up to date, sampling efforts have been made on both regions, but still it is not impossible to rule out that this apparent absence during certain times might be produced by a sampling artifact. Considering both records, below we evaluate several scenarios and hypotheses that attempt to explain the biogeographical history of Troodontidae in Europe:

a) *Troodontids reached the Ibero-Armorican island during the 'Dinosaur Turnover', around 70 m.a.* - This hypothesis assumes that the arrival of troodontid populations to the Ibero-Armorican island likely resulted from Laurasian (North American or Asian) dispersal events (Csiki-Sava et al., 2015; Ding et al., 2020; Sellés et al., 2021) and that they reached the island at the beginning of the posturnover interval. Thus, the uppermost Maastrichtian (C29r) troodontids from Ibero-Armorica were descendants of those that reached the island a few million years before, in the same dispersal pulse that brought the group from Asia or America to the Haţeg island in the lower Maastrichtian. Therefore, the arrival of troodontids on the Ibero-Armorican island would have occurred simultaneously with the migratory wave that introduced them to the eastern Haţeg island, and they would have reached the western island together with the Asian lambeosaurine hadrosaurids around 70 m.a (Prieto-Márquez et al., 2013; Conti et al., 2020). This possibility seems, however, quite improbable since there are no lambeosaurines known from the Haţeg island so far. Finally, in this hypothesis, the absence of troodontids in the Ibero-Armorican island during most of the Maastrichtian (and most of the post-turnover interval) would not be genuine absence, but perhaps be explained in terms of low sampling effort, sedimentary, or preservational biases. So far, no remains of troodontids have appeared in any of the localities sampled, and in this time interval (72–66.5 m.a.; mid-C31r-C30n) the theropod record is particularly scarce in all the Ibero-Armorican basins (with some Pyrenean basins even recording significant sedimentary hiatuses; Fondevilla et al., 2016). Furthermore, the number of troodontid remains identified so far from the uppermost Maastrichtian of the island is so low that we cannot completely rule out that remains of this clade will appear in the future in upper Maastrichtian levels older than C29r.
b) *Troodontids reached the Ibero-Armorican island late in the post-turnover interval, in the latest Maastrichtian, around 66.5 m.a.* - This hypothesis suggests that troodontids did not arrive during the faunal turnover, but they reached the Ibero-Armorican island in a later dispersal event. This dispersal event might have coincided with one of the marine regressions that occurred after the faunal turnover, such as the KMa5 event (Haq, 2014), which may have created available land bridges between the archipelago and the surrounding landmasses. Some authors (Martin et al., 2005; Brikiatis, 2014) proposed a terrestrial connection between North America and Europe, enabling faunal dispersal events during the late Maastrichtian. The high-latitude Thulean route (through Canadian islands and Greenland) could be the terrestrial corridor that brought marsupials to Europe in the late Maastrichtian, and the De Geer route (through Greenland and Fennoscandia) could have been an alternative connection between North America and western Europe in the latest Cretaceous. In any case, precise hypotheses about dispersal routes cannot be tested further until more complete and diagnostic theropod remains are recovered that determine a more precise phylogenetic affinity of the Ibero-Armorican troodontids. For instance, as we discussed above, it is not clear based on the dental records alone whether these Ibero-Armorican species are basal or derived troodontids, and these differing phylogenetic positions might imply vastly different dispersal histories.

5. Conclusions

Our review of isolated theropod teeth from the upper Maastrichtian Molí del Baró-1 locality in the southern Pyrenees (Catalonia, Spain) updates the taxonomy and diversity of the theropod assemblage of this fossil site and provides an important window into of the composition of theropod communities during the uppermost Maastrichtian (C29r) of Ibero-Armorica, during the final million years (or less) before the end-Cretaceous mass extinction. This non-avian theropod assemblage consists of small theropods, including velociraptorines, troodontids, and different undetermined dromaeosaurids (e.g., *Richardoestesia* and *Paronychodon*). Interestingly, the identification of a troodontid tooth, together with previous reports of troodontids from this region based on skeletal material (*Tamarro insperatus;* Sellés et al., 2021), corroborates the presence of the clade on the Ibero-Armorican island. Furthermore, based on our new analyses, we report the unusual occurrence of an undetermined dromaeosaurid tooth with striking affinities with microraptorines, a clade known almost exclusively from earlier in the Cretaceous in Asia. Microwear analysis shows that all studied teeth preserve a family of perpendicular to sub-perpendicular scratches (perpendicular to the longitudinal plane of the crown) that are probably related to a more specific and/or specialized feeding mechanism, being alternative or complementary to the typical 'puncture and pull' model of theropods. The microwear pattern observed in the troodontid suggests a certain degree of feeding specialization compared with the usual pattern of dromaeosaurids and close relatives, indicating an omnivorous diet with plants as a major component. Our reanalysis and review of these specimens underscores a high level of diversity in the upper Maastrichtian non-avian theropod assemblages of Europe and illuminates an end-Cretaceous ecosystem with abundant small theropods with different ecological niches. The Ibero-Armorican theropod assemblage at the end of the Cretaceous differs from those of the eastern Haţeg island and other assemblages worldwide, further illustrating how dinosaur faunas were regionally variable, diverse, and successful until the asteroid hit.

CRediT authorship contribution statement

Oscar Castillo-Visa: Writing – original draft, Conceptualization. **Mattia Antonio Baiano:** Writing – review & editing, Data curation. **Stephen L. Brusatte:** Writing – review & editing, Data curation. **Àngel Galobart:** Writing – review & editing, Resources, Funding acquisition. **Bernat Vila:** Writing – review & editing, Resources, Funding acquisition, Data curation.

Declaration of competing interest

The authors declare the following financial interests/personal relationships which may be considered as potential competing interests: Bernat Vila reports financial support was provided by Spain Ministry of Science and Innovation. Àngel Galobart reports financial support was provided by Generalitat de Catalunya Departament de Cultura i Mitjans de Comunicació. Bernat Vila reports a relationship with Institut Català de Paleontologia Miquel Crusafont that includes: employment and funding grants. Àngel Galobart reports a relationship with Institut Català de

Paleontologia Miquel Crusafont that includes: employment and funding grants. If there are other authors, they declare that they have no known competing financial interests or personal relationships that could have appeared to influence the work reported in this paper.

Acknowledgements

This research is part of the project VEBPI (reference R+D+i/PID2020- 119811GB-I00) funded by MCIN/AEI/10.13039/501100011033/. Additional funding was provided by the CERCA Programme and the project ARQ001SOL-173-2022 funded by the Departament de Cultura of the Generalitat de Catalunya. Bernat Vila and Àngel Galobart are members of the Consolidate Research Group 'Reptilian Ecosystems' [2021-SGR-01192]' approved by the Generalitat de Catalunya. The authors thank Jesús Felipe Serrano for motivating the development of present study, and Ferran Llorens for providing previous SEM images used for the wear analysis. Also, authors want to thank the four reviewers involved in the review process (Dr. Meso and anonymous) together with the Cretaceous Research's associated editor, Dr. Nicholas Longrich.

Data availability

Data will be made available on request.

References

Abreu Filho, W., Albuquerque, M.C., 2016. Projeto geologia das folhas Dom Aquino-Rondonópolis: estado de Mato Grosso. Serviço Geológico do Brasil - CPRM 1–178. Online version at: https://rigeo.sgb.gov.br/handle/doc/17709.

Baiano, M., Galobart, À., Dalla Vecchia, F.M., Vila, B., 2014. Aplicación de la microtomografía en el estudio de dientes aislados de dinosaurios terópodos. Proceedings of the XII Encuentro de Jóvenes Investigadores en Paleontología 9–12.

Barrett, P.M., Rayfield, E.J., 2006. Ecological and evolutionary implications of dinosaur feeding behaviour. Trends in Ecology & Evolution 21 (4), 217–224. https://doi.org/10.1016/j.tree.2006.01.002.

Barsbold, R., 1983. Carnivorous dinosaurs from the Cretaceous of Mongolia [in Russian]. Sovmestnaâ Sovetsko-Mongolskaâ Paleontologiceskaâ Ekspediciâ, Trudy 19, 1–117.

Barsbold, R., Osmólska, H., 1999. The skull of *Velociraptor* (Theropoda) from the Late Cretaceous of Mongolia. Acta Palaeontologica Polonica 44 (2), 189–219.

Bell, P.R., Currie, P.J., Russell, D.A., 2015. Large caenagnathids (Dinosauria, Oviraptorosauria) from the uppermost Cretaceous of western Canada. Cretaceous Research 52, 101–107. https://doi.org/10.1016/j.cretres.2014.09.006.

Bonaparte, J.F., 1985. A horned Cretaceous carnosaur from Patagonia. National Geographic Research 1, 149–151.

Brikiatis, L., 2014. The De Geer, Thulean and Beringia routes: key concepts for understanding early Cenozoic biogeography. Journal of Biogeography 41 (6), 1036–1054. https://doi.org/10.1111/jbi.12310.

Brum, A.S., Pegas, R.V., Bandeira, K.L., Souza, L.G., Campos, D.A., Kellner, A.W., 2021. A new unenlagiine (Theropoda, Dromaeosauridae) from the Upper Cretaceous of Brazil. Papers in Palaeontology 7 (4), 2075–2099. https://doi.org/10.1002/spp2.1375.

Brusatte, S.L., Vremir, M., Csiki-Sava, Z., Turner, A.H., Watanabe, A., Erickson, G.M., Norell, M.A., 2013. The osteology of *Balaur bondoc*, an island-dwelling dromaeosaurid (Dinosauria: Theropoda) from the Late Cretaceous of Romania. Bulletin of the American Museum of Natural History 2013 (374), 1–100. https://doi.org/10.1206/798.1.

Brusatte, S.L., Candeiro, C.R.A., Simbras, F.M., 2017. The last dinosaurs of Brazil: The Bauru Group and its implications for the end-Cretaceous mass extinction. Annals of the Brazilian Academy of Sciences 89, 1465–1485. https://doi.org/10.1590/0001-3765201720160918.

Candeiro, C.R.A., Santos, A.R., Bergqvist, L.P., Ribeiro, L.C.B., Apesteguía, S., 2008. The Late Cretaceous fauna and flora of the Uberaba area (Minas Gerais State, Brazil). Journal of South American Earth Sciences 25 (2), 203–216. https://doi.org/10.1016/j.jsames.2007.06.005.

Canudo, J.I., Barco, J.L., Cruzado-Caballero, P., Cuenca-Bescós, G., Ruiz-Omeñaca, J.I., Royo-Torres, R., 2005. Evidencias de predación de dinosaurios terópodos en el Maastrichtiense superior: cretácico superior de Arén (Huesca). Lucas Mallada: Revista de ciencias 12, 29–58.

Canudo, J.I., Oms, O., Vila, B., Galobart, À., Fondevilla, V., Puértolas-Pascual, E., Sellés, A.G., Cruzado-Caballero, P., Dinarès-Turell, J., Vicens, E., Castanera, D., Company, J., Burrel, L., Estrada, R., Marmi, J., Blanco, A., 2016. The Upper Maastrichtian dinosaur fossil record from the southern Pyrenees and its contribution to the topic of the Cretaceous–Palaeogene mass extinction event. Cretaceous Research 57, 540–551. https://doi.org/10.1016/j.cretres.2015.06.013.

Cau, A., 2024. A Unified Framework for Predatory Dinosaur Macroevolution. Bollettino della Societa Paleontologica Italiana 63 (1), 1–19. https://doi.org/10.4435/BSPI.2024.08.

Cau, A., Brougham, T., Naish, D., 2015. The phylogenetic affinities of the bizarre Late Cretaceous Romanian theropod *Balaur bondoc* (Dinosauria, Maniraptora): dromaeosaurid or flightless bird? PeerJ 3, e1032. https://doi.org/10.7717/peerj.1032.

Claessens, L.P., Loewen, M.A., 2016. A redescription of *Ornithomimus velox* Marsh, 1890 (Dinosauria, Theropoda). Journal of Vertebrate Paleontology 36 (1), e1034593. https://doi.org/10.1080/02724634.2015.1034593.

Clyde, W.C., Krause, J.M., De Benedetti, F., Ramezani, J., Cúneo, N.R., Gandolfo, M.A., Haber, P., Whelan, C., Smith, T., 2021. New South American record of the Cretaceous–Paleogene boundary interval (La Colonia Formation, Patagonia, Argentina). Cretaceous Research 126, 104889. https://doi.org/10.1016/j.cretres.2021.104889.

Codrea, V., Smith, T., Dica, P., Folie, A., Garcia, G., Godefroit, P., Van Itterbeeck, J., 2002. Dinosaur egg nests, mammals and other vertebrates from a new Maastrichtian site of the Haţeg Basin (Romania). Comptes Rendus Palevol 1 (3), 173–180. https://doi.org/10.1016/S1631-0683(02)00021-0.

Conti, S., Vila, B., Sellés, A.G., Galobart, À., Benton, M.J., Prieto-Márquez, A., 2020. The oldest lambeosaurine dinosaur from Europe: insights into the arrival of Tsintaosaurini. Cretaceous Research 107, 104286. https://doi.org/10.1016/j.cretres.2019.104286.

Csiki, Z., Grigorescu, D., 1998. Small theropods from the late cretaceous of the HAŢEG basin (Western Romania). An unexpected diversity at the top of the food chain. Oryctos 1, 87–104.

Csiki, Z., Vremir, M., Brusatte, S.L., Norell, M.A., 2010. An aberrant island-dwelling theropod dinosaur from the Late Cretaceous of Romania. Proceedings of the National Academy of Sciences 107 (35), 15357–15361. https://doi.org/10.1073/pnas.1006970107.

Csiki-Sava, Z., Buffetaut, E., Ősi, A., Pereda-Suberbiola, X., Brusatte, S.L., 2015. Island life in the Cretaceous-faunal composition, biogeography, evolution, and extinction of land-living vertebrates on the Late Cretaceous European archipelago. ZooKeys 469, 1–161. https://doi.org/10.3897/zookeys.469.8439.

Csiki-Sava, Z., Vremir, M., Vasile, Ş., Brusatte, S.L., Dyke, G., Naish, D., Norell, M.A., Totoianu, R., 2016. The east side story–the Transylvanian latest Cretaceous continental vertebrate record and its implications for understanding Cretaceous– Paleogene boundary events. Cretaceous Research 57, 662–698. https://doi.org/10.1016/j.cretres.2015.09.003.

Cullen, T.M., Cousens, B.L., 2023. New biogeochemical insights into Mesozoic terrestrial paleoecology and evidence for omnivory in troodontid dinosaurs. Geological Society of America Bulletin. https://doi.org/10.1130/B37077.1.

Currie, P.J., Evans, D.C., 2020. Cranial anatomy of new specimens of *Saurornitholestes langstoni* (Dinosauria, Theropoda, Dromaeosauridae) from the dinosaur park formation (Campanian) of Alberta. The Anatomical Record 303 (4), 691–715. https://doi.org/10.1002/ar.24241.

Currie, P.J., Rigby Jr, J.K., Sloan, R.E., 1990. Theropod teeth from the Judith River formation of southern Alberta, Canada. In: Carpenter, K., Currie, P. (Eds.), Dinosaur Systematics: Perspectives and Approaches. Cambridge University Press, pp. 107–125.

DePalma, R.A., Burnham, D.A., Martin, L.D., Larson, P.L., Bakker, R.T., 2015. The first giant raptor (Theropoda: Dromaeosauridae) from the hell creek formation. Paleontological Contributions 2015 (14), 1–16. https://doi.org/10.17161/paleo.1808.18764.

Dias-Brito, D., Musacchio, E.A., Castro, J.D., Maranhão, M.S., Suárez, J.M., Rodrigues, R., 2001. Grupo Bauru: uma unidade continental do Cretáceo no Brasil-concepções baseadas em dados micropaleontológicos, isotópicos e estratigráficos. Revue de Paléobiologie 20 (1), 245–304.

Ding, A., Pittman, M., Upchurch, P., O'Connor, J., Field, D.J., Xu, X., 2020. The biogeography of coelurosaurian theropods and its impact on their evolutionary history. Bulletin of the American Museum of Natural History 40 (440), 117–157.

Ezcurra, M.D., Agnolín, F.L., 2012. A new global palaeobiogeographical model for the late Mesozoic and early Tertiary. Systematic Biology 61 (4), 553–566. https://doi.org/10.1093/sysbio/syr115.

Fiorillo, A.R., 1998. Dental microwear patterns of the sauropod dinosaurs *Camarasaurus* and *Diplodocus*: evidence for resource partitioning in the Late Jurassic of North America. Historical Biology 13 (1), 1–16.

Fiorillo, A.R., 2008. On the occurrence of exceptionally large teeth of *Troodon* (Dinosauria: Saurischia) from the Late Cretaceous of northern Alaska. PALAIOS 23 (5), 322–328. https://doi.org/10.2110/palo.2007.p07-036r.

Fondevilla, V., Dinarès-Turell, J., Oms, O., 2016. The chronostratigraphic framework of the South-Pyrenean Maastrichtian succession reappraised: Implications for basin development and end-Cretaceous dinosaur faunal turnover. Sedimentary Geology 337, 55–68. https://doi.org/10.1016/j.sedgeo.2016.03.006.

Fondevilla, V., Riera, V., Vila, B., Sellés, A.G., Dinarès-Turell, J., Vicens, E., Gaete, R., Oms, O., Galobart, A., 2019. Chronostratigraphic synthesis of the latest Cretaceous dinosaur turnover in south-western Europe. Earth-Science Reviews 191, 168–189. https://doi.org/10.1016/j.earscirev.2019.01.007.

Fowler, D.W., Wilson, J.P., Fowler, E.A.F., Noto, C.R., Anduza, D., Horner, J.R., 2020. *Trierarchuncus prairiensis* gen. et sp. nov., the last alvarezsaurid: Hell Creek Formation (uppermost Maastrichtian), Montana. Cretaceous Research 116, 104560. https://doi.org/10.1016/j.cretres.2020.104560.

Frederickson, J.A., Engel, M.H., Cifelli, R.L., 2018. Niche partitioning in theropod dinosaurs: Diet and habitat preference in predators from the Uppermost Cedar Mountain Formation (Utah, USA). Scientific Reports 8 (1), 17872. https://doi.org/10.1038/s41598-018-35689-6.

Funston, G.F., Mendonca, S.E., Currie, P.J., Barsbold, R., 2018. Oviraptorosaur anatomy, diversity and ecology in the Nemegt Basin. Palaeogeography, Palaeoclimatology, Palaeoecology 494, 101–120. https://doi.org/10.1016/j.palaeo.2017.10.023.

Gates, T.A., Zanno, L.E., Makovicky, P.J., 2013. Theropod teeth from the upper Maastrichtian Hell Creek Formation "Sue" Quarry: New morphotypes and faunal comparisons. Acta Palaeontologica Polonica 60 (1), 131–139. https://doi.org/10.4202/app.2012.0145.

Gilmore, C.W., 1924. On *Troodon validus*, an ornithopodous dinosaur from the Belly River Formation (Cretaceous). In: Alberta. Canadian Bulletin, 1. Department of Geology, University of Alberta, pp. 1–143.

Godefroit, P., Golovneva, L., Shchepetov, S., Garcia, G., Alekseev, P., 2009. The last polar dinosaurs: high diversity of latest Cretaceous arctic dinosaurs in Russia. Naturwissenschaften 96, 495–501. https://doi.org/10.1007/s00114-008-0499-0.

Goloboff, P.A., 1999. Analyzing large data sets in reasonable times: Solutions for composite optima. Cladistics 15, 415–428.

Goloboff, P.A., Morales, M.F., 2023. TNT version 1.6, with a graphical interface for MacOS and Linux, including new routines in parallel. Cladistics 39, 144–153. https://doi.org/10.1111/cla.12524.

Goswami, A., Prasad, G.V.R., Verma, O., Flynn, J.J., Benson, R.B.J., 2013. A troodontid dinosaur from the latest Cretaceous of India. Nature Communications 4 (1), 1703. https://doi.org/10.1038/ncomms2716.

Gauthier, J., 1986. Saurischian monophyly and the origin of birds. California Academy of Sciences, Memoirs 8, 1–55.

Gheerbrant, E., Rage, J.C., 2006. Paleobiogeography of Africa: how distinct from Gondwana and Laurasia? Palaeogeography, Palaeoclimatology, Palaeoecology 241 (2), 224–246. https://doi.org/10.1016/j.palaeo.2006.03.016.

Haq, B.U., 2014. Cretaceous eustasy revisited. Global and Planetary Change 113, 44–58. https://doi.org/10.1016/j.gloplacha.2013.12.007.

Han, F., Wang, Q., Wang, H., Zhu, X., Zhou, X., Wang, Z., Fang, K., Stidham, T.A., Wang, W., Wang, X., Li, X., Qin, H., Fan, L., Wen, C., Luo, J., Pan, Y., Deng, C., 2022. Low dinosaur biodiversity in central China 2 million years prior to the end-Cretaceous mass extinction. Proceedings of the National Academy of Sciences 119 (39), e2211234119. https://doi.org/10.1073/pnas.221123411.

Hendrickx, C., Mateus, O., 2014. Abelisauridae (Dinosauria: Theropoda) from the Late Jurassic of Portugal and dentition-based phylogeny as a contribution for the identification of isolated theropod teeth. Zootaxa 3759. https://doi.org/10.11646/zootaxa.3759.1.1.

Hendrickx, C., Mateus, O., Araújo, R., 2015. A proposed terminology of theropod teeth (Dinosauria, Saurischia). Journal of Vertebrate Paleontology 35 (5), e982797. https://doi.org/10.1080/02724634.2015.982797.

Hendrickx, C., Mateus, O., Araujo, R., Choiniere, J., 2019. The distribution of dental features in non-avian theropod dinosaurs: Taxonomic potential, degree of homoplasy, and major evolutionary trends. Palaeontologia Electronica 22 (3), 1–110. https://doi.org/10.26879/820.

Hendrickx, C., Tschopp, E., D Ezcurra, M., 2020. Taxonomic identification of isolated theropod teeth: the case of the shed tooth crown associated with *Aerosteon* (Theropoda: Megaraptora) and the dentition of Abelisauridae. Cretaceous Research 108, 104312. https://doi.org/10.1016/j.cretres.2019.104312.

Holtz, T.R., Brinkman, D.L., Chandler, C.H., 1998. Denticle morphometric and a possibly omnivorous feeding habit for the theropod dinosaur T*roodon*. GAIA 15, 159–166.

Horner, J.R., Goodwin, M.B., Myhrvold, N., 2011. Dinosaur census reveals abundant *Tyrannosaurus* and rare ontogenetic stages in the Upper Cretaceous Hell Creek Formation (Maastrichtian), Montana, USA. PLoS One 6 (2), e16574. https://doi.org/10.1371/journal.pone.0016574.

Hwang, S.H., 2005. Phylogenetic patterns of enamel microstructure in dinosaur teeth. Journal of Morphology 266 (2), 208–240. https://doi.org/10.1002/jmor.10372.

Isasmendi, E., Torices, A., Canudo, J.I., Currie, P.J., Pereda-Suberbiola, X., 2022. Upper Cretaceous European theropod palaeobiodiversity, palaeobiogeography and the intra-Maastrichtian faunal turnover: new contributions from the Iberian fossil site of Laño. Papers in Palaeontology 8 (1), e1419. https://doi.org/10.1002/spp2.1419.

Isasmendi, E., Pérez-Pueyo, M., Moreno-Azanza, M., Alonso, A., Puértolas-Pascual, E., Bádenas, B., Canudo, J.I., 2024. Theropod teeth palaeodiversity from the uppermost cretaceous of the South Pyrenean Basin (NE Iberia) and the intra- Maastrichtian faunal turnover. Cretaceous Research, 105952. https://doi.org/10.1016/j.cretres.2024.105952.

Iori, F.V., de Araújo-Júnior, H.I., Tavares, S.A.S., da Silva Marinho, T., Martinelli, A.G., 2021. New theropod dinosaur from the Late Cretaceous of Brazil improves abelisaurid diversity. Journal of South American Earth Sciences 112, 103551. https://doi.org/10.1016/j.jsames.2021.103551.

Jasinski, S.E., Sullivan, R.M., Dodson, P., 2020. New dromaeosaurid dinosaur (Theropoda, Dromaeosauridae) from New Mexico and biodiversity of dromaeosaurids at the end of the Cretaceous. Scientific Reports 10 (1), 5105. https://doi.org/10.1038/s41598-020-61480-7.

Kane, A., Healy, K., Ruxton, G.D., Jackson, A.L., 2016. Body size as a driver of scavenging in theropod dinosaurs. The American Naturalist 187 (6), 706–716. https://doi.org/10.1086/686094.

Kessler, E., Grigorescu, D., Csiki, Z., 2005. *Elopteryx* revisited-a new bird-like specimen from the Maastrichtian of the Haţeg Basin (Romania). Acta Palaeontologica Romaniae 5, 249–258.

Lamanna, M.C., Sues, H.D., Schachner, E.R., Lyson, T.R., 2014. A new large-bodied oviraptorosaurian theropod dinosaur from the latest Cretaceous of western North America. PLoS One 9 (3), e92022. https://doi.org/10.1371/journal.pone.0092022.

Larson, D.W., 2008. Diversity and variation of theropod dinosaur teeth from the uppermost Santonian Milk River Formation (Upper Cretaceous), Alberta: a quantitative method supporting identification of the oldest dinosaur tooth assemblage in Canada. Canadian Journal of Earth Sciences 45 (12), 1455–1468. https://doi.org/10.1139/e08-070.

Larson, D.W., Currie, P.J., 2013. Multivariate analyses of small theropod dinosaur teeth and implications for paleoecological turnover through time. PLoS One 8 (1), e54329. https://doi.org/10.1371/journal.pone.0054329.

Larson, D.W., Brinkman, D.B., Bell, P.R., 2010. Faunal assemblages from the upper Horseshoe Canyon Formation, an early Maastrichtian cool-climate assemblage from Alberta, with special reference to the *Albertosaurus sarcophagus* bonebed. Canadian Journal of Earth Sciences 47 (9), 1159–1181. https://doi.org/10.1139/E10-005.

Larson, D.W., Brown, C.M., Evans, D.C., 2016. Dental disparity and ecological stability in bird-like dinosaurs prior to the end-Cretaceous mass extinction. Current Biology 26 (10), 1325–1333. https://doi.org/10.1016/j.cub.2016.03.039.

Laurent, Y., 2002. Les faunes de vertébrés du Maastrichtien supérieur d'Europe: systématique et biodiversité, vol. III. Université Paul-Sabatier - Toulussé, p. 214 (PhD dissertation, Strata, série 2. 41.

Le Loeuff, J., 1992. Les vertébrés continentaux du Crétacé supérieur d'Europe: Paléoecologie, Biostratigraphie et Paléobiogeographie (PhD dissertation, Mémoires des Sciences de la Terre). Université Pierré et Marie Curie, Paris, p. 271.

Le Loeuff, J., Buffetaut, E., Martin, M., 1994. The last stages of dinosaur faunal history in Europe: a succession of Maastrichtian dinosaur assemblages from the Corbières (southern France). Geological Magazine 131 (5), 625–630. https://doi.org/10.1017/S0016756800012413.

Li, Z., Wang, C.C., Wang, M., Chiang, C.C., Wang, Y., Zheng, X., Huang, E., Hsiao, K., Zhou, Z., 2020. Ultramicrostructural reductions in teeth: implications for dietary transition from non-avian dinosaurs to birds. BMC Evolutionary Biology 20, 1–8. https://doi.org/10.1186/s12862-020-01611-w.

Longrich, N., 2008. Small theropod teeth from the Lance Formation of Wyoming, USA (Chapter 9). In: Sankey, J.T., Baszio, S. (Eds.), Vertebrate microfossil assemblages: Their role in paleoecology and paleobiogeography. Indiana University Press, Bloomington, pp. 135–158.

Longrich, N.R., Currie, P.J., 2009. A microraptorine (Dinosauria–Dromaeosauridae) from the late Cretaceous of North America. Proceedings of the National Academy of Sciences 106 (13), 5002–5007. https://doi.org/10.1073/pnas.0811664106.

Longrich, N.R., Pereda-Suberbiola, X., Jalil, N.E., Khaldoune, F., Jourani, E., 2017. An abelisaurid from the latest Cretaceous (late Maastrichtian) of Morocco, North Africa. Cretaceous Research 76, 40–52. https://doi.org/10.1016/j.cretres.2017.03.021.

Longrich, N.R., Isasmendi, E., Pereda-Suberbiola, X., Jalil, N.E., 2023. New fossils of Abelisauridae (Dinosauria: Theropoda) from the upper Maastrichtian of Morocco, North Africa. Cretaceous Research 152, 105677. https://doi.org/10.1016/j.cretres.2023.105677.

López-Martínez, N., Vicens, E., 2012. A new peculiar dinosaur egg, *Sankofa pyrenaica* oogen. nov. oosp. nov. from the Upper Cretaceous coastal deposits of the Aren Formation, south-central Pyrenees, Lleida, Catalonia, Spain. Palaeontology 55 (2), 325–339. https://doi.org/10.1111/j.1475-4983.2011.01114.x.

Lü, J., Xu, L., Liu, Y., Zhang, X., Jia, S., Ji, Q., 2010. A new troodontid theropod from the Late Cretaceous of central China, and the radiation of Asian troodontids. Acta Palaeontologica Polonica 55 (3), 381–388. https://doi.org/10.4202/app.2009.0047.

Lü, J.C., Xu, L., Chang, H.L., Jia, S.H., Zhang, J.M., Gao, D.S., Zhang, Y.Y., Zhang, C.J., Ding, F., 2018. A new alvarezsaurid dinosaur from the Late Cretaceous Qiupa Formation of Luanchuan, Henan Province, central China. China Geology 1 (1), 28–35. https://doi.org/10.31035/cg2018005.

Maddison, W.P., Maddison, D.R., 2019. Mesquite: A modular system for evolutionary analysis.

Makovicky, P.J., Norell, M.A., Clark, J.M., Rowe, T., 2003. Osteology and relationships of *Byronosaurus jaffei* (Theropoda: Troodontidae). American Museum Novitates 3402, 1–32. https://doi.org/10.1206/0003-0082(2003)402%3C0001:oarobj%3E2.0.co;2.

Malafaia, E., Escaso, F., Coria, R.A., Ortega, F., 2023. An Eudromaeosaurian Theropod from Lo Hueco (Upper Cretaceous. Central Spain). Diversity 15 (2), 141. https://doi.org/10.3390/d15020141.

Malafaia, E., Escaso, F., Coria, R.A., Pérez-García, A., Ortega, F., 2025. Theropod teeth from the Upper Cretaceous of central Spain: Assessing the paleobiogeographic history of European abelisaurids. Cretaceous Research 168, 106072. https://doi.org/10.1016/j.cretres.2024.106072.

Mallon, J.C., Anderson, J.S., 2014. The functional and palaeoecological implications of tooth morphology and wear for the megaherbivorous dinosaurs from the Dinosaur Park Formation (Upper Campanian) of Alberta, Canada. PLoS one 9 (6), e98605. https://doi.org/10.1371/journal.pone.0098605.

Maranga, D.C.A., 2021. Detailed Morphology of the Skull and Dentition in a New, Exceptionally Preserved Microraptorine Specimen (Theropoda: Dromaeosauridae) from the Early Cretaceous of China (Unpubl. Master's dissertation). University of Toronto, Canada, p. 87.

Marmi, J., Blanco, A., Fondevilla, V., Dalla Vecchia, F.M., Sellés, A.G., Vicente, A., Martín-Closas, C., Oms, O., Galobart, A., 2016. The Molí del Baró-1 site, a diverse fossil assemblage from the uppermost Maastrichtian of the southern Pyrenees (north-eastern Iberia). Cretaceous Research 57, 519–539. https://doi.org/10.1016/j.cretres.2015.06.016.

Marsh, O.C., 1881. Principal characters of American Jurassic dinosaurs, part V. American Journal of Science 3 (125), 417–423.

Martin, J.E., Case, J.A., Jagt, J.W., Schulp, A.S., Mulder, E.W., 2005. A new European marsupial indicates a Late Cretaceous high-latitude transatlantic dispersal route. Journal of Mammalian Evolution 12, 495–511. https://doi.org/10.1007/s10914-005-7330-x.

Matthew, W.D., Brown, B., 1922. The family Deinodontidae, with notice of a new genus from the Cretaceous of Alberta. American Museum of Natural History Bulletin 46, 367–385.

Meso, J.G., Hendrickx, C., Baiano, M.A., Canale, J.I., Salgado, L., Díaz-Martínez, I., 2021. Isolated theropod teeth associated with a sauropod skeleton from the Late Cretaceous Allen Formation of Río Negro, Patagonia, Argentina. Acta Palaeontologica Polonica 66, 409–423. https://doi.org/10.4202/app.00847.2020.

Meso, J.G., Gianechini, F.A., Valieri, R.J., Apesteguía, S., Correa, S.A.S., 2022. Theropods from the La Bonita site, Bajo de la Carpa Formation (Neuquén Group, Santonian), Río Negro, Argentina: analysis of dental evidence. Cretaceous Research 137, 105250. https://doi.org/10.1016/j.cretres.2022.105250.

Meso, J.G., Gianechini, F., Gomez, K.L., Muci, L., Baiano, M.A., Pol, D., Kaluza, J., Garrido, A., Pittman, M., 2024. Shed teeth from Portezuelo formation at Sierra del Portezuelo reveal a higher diversity of predator theropods during Turonian- Coniacian times in northern Patagonia. BMC Ecology and Evolution 24 (1), 59. https://doi.org/10.1186/s12862-024-02249-8.

Mohabey, D.M., Samant, B., Vélez-Rosado, K.I., Wilson Mantilla, J.A., 2024. A review of small-bodied theropod dinosaurs from the Upper Cretaceous of India, with description of new cranial remains of a noasaurid (Theropoda: Abelisauria). Journal of Vertebrate Paleontology, e2288088. https://doi.org/10.1080/02724634.2023.2288088.

Motta, M.J., 2023. Anatomía comparada de los terópodos paravianos Unenlagiidae y sus implicancias en el origen de las aves (PhD dissertation). Universidad Nacional de La Plata, La Plata, p. 411.

Naish, D., Dyke, G.J., 2004. *Heptasteornis* was no ornithomimid, troodontid, dromaeosaurid or owl: the first alvarezsaurid (Dinosauria: Theropoda) from Europe. Neues Jahrbuch fur Geologie und Palaontologie Monatshefte 7, 385–401. https://doi.org/10.1127/njgpm/2004/2004/385.

Nixon, K.C., 1999. The parsimony ratchet, a new method for rapid parsimony analysis. Cladistics 15, 407–414.

Norell, M.A., Makovicky, P.J., Bever, G.S., Balanoff, A.M., Clark, J.M., Barsbold, R., Rowe, T., 2009. A review of the Mongolian Cretaceous dinosaur *Saurornithoides* (Troodontidae: Theropoda). American Museum Novitates 3654, 1–63. https://doi.org/10.1206/648.1.

Novas, F., Ribeiro, L.C.B., de Souza Carvalho, I., 2005. Maniraptoran theropod ungual from the Marília Formation (Upper Cretaceous), Brazil. Revista del Museo Argentino de Ciencias Naturales Nueva Serie 7 (1), 37–41.

Novas, F.E., de Souza Carvalho, I., Ribeiro, L.C.B., Méndez, A.H., 2008. First abelisaurid bone remains from the Maastrichtian Marilia Formation, Bauru basin, Brazil. Cretaceous Research 29 (4), 625–635. https://doi.org/10.1016/j.cretres.2008.01.010.

Novas, F.E., Chatterjee, S., Rudra, D.K., Datta, P., 2010. *Rahiolisaurus gujaratensis*, n. gen. n. sp., A New Abelisaurid Theropod from the Late Cretaceous of India (Chapter 3). In: Bandyopadhyay, S. (Ed.), New Aspects of Mesozoic Biodiversity. Lecture Notes in Earth Sciences, vol. 132. Springer, Heidelberg, pp. 45–62. https://doi.org/10.1007/978-3-642-10311-7_3.

Ortega, F., Bardet, N., Barroso-Barcenilla, F., Callapez, P.M., Cambra-Moo, O., Daviero-Gómez, V., Díez Díaz, V., Domingo, L., Elvira, A., Escaso, F., García-Oliva, M., Gómez, B., Houssaye, A., Knoll, F., Marcos-Fernández, F., Martín, M., Mocho, P., Narváez, I., Pérez-García, A., Peyrot, D., Segura, M., Serrano, H., Torices, A., Vidal, D., Sanz, J.L., 2015. The biota of the Upper Cretaceous site of Lo Hueco (Cuenca, Spain). Journal of Iberian Geology 41 (1), 83–99. https://doi.org/10.5209/rev_JIGE.2015.v41.n1.48657.

Ősi, A., Apesteguía, S., Kowalewski, M., 2010. Non-avian theropod dinosaurs from the early Late Cretaceous of Central Europe. Cretaceous Research 31 (3), 304–320. https://doi.org/10.1016/j.cretres.2010.01.001.

Ősi, A., Szabó, M., Kollmann, H., Wagreich, M., Kalmar, R., Makádi, L., Szentesi, Z., Summesberger, H., 2019. Vertebrate remains from the Turonian (Upper Cretaceous) Gosau Group of Gams, Austria. Cretaceous Research 99, 190–208. https://doi.org/10.1016/j.cretres.2019.03.001.

Owen, R., 1842. Report on British fossil reptiles, Part II. Reports of the British Association for the. Advancement of Science 11, 60–204.

Pereda-Suberbiola, X., 2009. Biogeographical affinities of Late Cretaceous continental tetrapods of Europe: a review. Bulletin de la Societe Geologique de France 180 (1), 57–71. https://doi.org/10.2113/gssgfbull.180.1.57.

Pérez-Pueyo, M.P., Pascual, E.P., Sanagustín, J.I.C., Lago, B.B., 2019. Larra 4: desenterrando a los últimos vertebrados del Maastrichtiense terminal del Pirineo aragonés. Zubia 31, 175–180.

Pérez-Pueyo, M., Cruzado-Caballero, P., Moreno-Azanza, M., Vila, B., Castanera, D., Gasca, J.M., Puértolas-Pascual, E., Badenas, B., Canudo, J.I., 2021. The tetrapod fossil record from the uppermost Maastrichtian of the Ibero-Armorican Island: An integrative review based on the outcrops of the western Tremp Syncline (Aragón, Huesca Province, NE Spain). Geosciences 11 (4), 162. https://doi.org/10.3390/geosciences11040162.

Pol, D., Baiano, M.A., Černý, D., Novas, F.E., Cerda, I.A., Pittman, M., 2024. A new abelisaurid dinosaur from the end Cretaceous of Patagonia and evolutionary rates among the Ceratosauria. Cladistics. https://doi.org/10.1111/cla.12583.

Prasad, G.V., Verma, V., Grover, P., Priyadarshini, R., Sahni, A., Lourembam, R.S., 2016. Isolated Archosaur teeth from the green sandstone capping the Coralline Limestone (Bagh Group) of the Narmada valley: Evidence for the presence of pre- Late to Late Maastrichtian abelisaurids in India. Island Arc 25 (6), 410–420. https://doi.org/10.1111/iar.12142.

Prieto-Márquez, A., Gaete, R., Galobart, A., Ardévol, L., 2000. A *Richardoestesia*-like theropod tooth from the Late Cretaceous foredeep, south-central Pyrenees, Spain. Eclogae Geologicae Helvetiae 93 (3), 497–502.

Prieto-Márquez, A., Dalla Vecchia, F.M., Gaete, R., Galobart, À., 2013. Diversity, relationships, and biogeography of the lambeosaurine dinosaurs from the European Archipelago, with description of the new aralosaurin *Canardia garonnensis*. PLoS One 8 (7), e69835. https://doi.org/10.1371/journal.pone.0069835.

Puértolas-Pascual, E., Arenillas, I., Arz, J.A., Calvín, P., Ezquerro, L., García-Vicente, C., Pérez-Pueyo, M., Sánchez-Moreno, E.M., Villalaín, J.J., Canudo, J. I., 2018. Chronostratigraphy and new vertebrate sites from the upper Maastrichtian of Huesca (Spain), and their relation with the K/Pg boundary. Cretaceous Research 89, 36–59. https://doi.org/10.1016/j.cretres.2018.02.016.

Rauhut, O.W., 2002. Dinosaur teeth from the Barremian of Uña, province of Cuenca, Spain. Cretaceous Research 23 (2), 255–263. https://doi.org/10.1006/cres.2002.1003.

Russell, D.A., Russell, D.E., Sweet, A.R., 1993. The end of the dinosaurian era in the Nanxiong Basin. Vertebrata Palasiatica 31 (2), 139–145.

Sankey, J.T., 2008. Diversity of latest Cretaceous (late Maastrichtian) small theropods and birds: teeth from the Lance and Hell Creek formations, USA. In: Sankey, J.T., Baszio, S. (Eds.), Vertebrate microfossil assemblages: Their role in paleoecology and paleobiogeography. Indiana University Press, Bloomington, pp. 117–134.

Sankey, J.T., Brinkman, D.B., Guenther, M., Currie, P.J., 2002. Small theropod and bird teeth from the late Cretaceous (late Campanian) Judith River Group, Alberta. Journal of Paleontology 76 (4), 751–763. https://doi.org/10.1666/0022-3360(2002)076<0751:STABTF>2.0. CO;2.

Scotese, C.R., 2014. Atlas of Late Cretaceous paleogeographic maps, PALEOMAP atlas for ArcGIS, volume 2, The Cretaceous, Maps 16–22, Mollweide Projection. ResearchGate Academia 2. https://doi.org/10.13140/2.1.4691.3284.

Seeley, H.G., 1888. Classification of the dinosauria. Geological Magazine 5 (1), 45–46. https://doi.org/10.1017/S0016756800156006.

Sellés, A.G., Vila, B., Galobart, A., 2014. Diversity of theropod ootaxa and its implications for the latest Cretaceous dinosaur turnover in southwestern Europe. Cretaceous Research 49, 45–54. https://doi.org/10.1016/j.cretres.2014.02.004.

Sellés, A.G., Vila, B., Brusatte, S.L., Currie, P.J., Galobart, À., 2021. A fast-growing basal troodontid (Dinosauria: Theropoda) from the latest Cretaceous of Europe. Scientific Reports 11 (1), 1–12. https://doi.org/10.1038/s41598-021-83745-5.

Sereno, P.C., 1997. The origin and evolution of dinosaurs. Annual Review of Earth and Planetary Sciences 25 (1), 435–489. https://doi.org/10.1146/annurev.earth.25.1.435.

Stein, W.W., 2019. Taking count: a census of dinosaur fossils recovered from the Hell Creek and Lance Formations (Maastrichtian). Journal of Paleontological Sciences 8, 1–42.

Sues, H.D., Averianov, A., 2013. Enigmatic teeth of small theropod dinosaurs from the Upper Cretaceous (Cenomanian–Turonian) of Uzbekistan. Canadian Journal of Earth Sciences 50 (3), 306–314. https://doi.org/10.1139/e2012-033.

Sweetman, S.C., 2004. The first record of velociraptorine dinosaurs (Saurischia, Theropoda) from the Wealden (Early Cretaceous, Barremian) of southern England. Cretaceous Research 25 (3), 353–364. https://doi.org/10.1016/j.cretres.2004.01.004.

Torices, A., Currie, P.J., Canudo, J.I., Pereda-Suberbiola, X., 2015. Theropod dinosaurs from the Upper Cretaceous of the South Pyrenees Basin of Spain. Acta Palaeontologica Polonica 60 (3), 611–626. https://doi.org/10.4202/app.2012.0121.

Torices, A., Wilkinson, R., Arbour, V.M., Ruiz-Omeñaca, J.I., Currie, P.J., 2018. Puncture-and-pull biomechanics in the teeth of predatory coelurosaurian dinosaurs. Current Biology 28 (9), 1467–1474. https://doi.org/10.1016/j.cub.2018.03.042.

Tortosa, T., Buffetaut, E., Vialle, N., Dutour, Y., Turini, E., Cheylan, G., 2014. A new abelisaurid dinosaur from the Late Cretaceous of southern France: Palaeobiogeographical implications. Annales de Paléontologie 100 (1), 63–86. https://doi.org/10.1016/j.annpal.2013.10.003.

Tschopp, E., Barta, D.E., Brinkmann, W., Foster, J.R., Holwerda, F.M., Maidment, S.C. R., Poropat, S.F., Scheyer, T.M., Sellés, A.G., Vila, B., Zahner, M., 2020. How to Live with Dinosaurs: Ecosystems Across the Mesozoic (Chapter 8). In: Martinetto, E., Tschopp, E., Gastaldo, R.A. (Eds.), Nature through Time. Springer Textbooks in Earth Sciences, Geography and Environment. Springer, Cham. https://doi.org/10.1007/978-3-030-35058-1_8.

Tumanova, T.A., Bolotsky Yu, L., Alifanov, V.R., 2004. The first finds of armored dinosaurs in the Upper Cretaceous of Russia (Amur Region). Paleontological Journal 38 (1), 73–77.
Turner, A.H., Hwang, S.H., Norell, M.A., 2007. A small derived theropod from Öösh, early Cretaceous, Baykhangor Mongolia. American Museum Novitates 3557, 1–27. https://doi.org/10.1206/0003-0082(2007)3557[1:ASDTFS]2.0. CO;2.
Turner, A.H., Makovicky, P.J., Norell, M.A., 2012. A review of dromaeosaurid systematics and paravian phylogeny. Bulletin of the American Museum of Natural History 2012 (371), 1–206. https://doi.org/10.1206/748.1.
Vianey-Liaud, M., Lopez-Martinez, N., 1997. Late Cretaceous dinosaur eggshells from the Tremp basin, southern Pyrenees, Lleida, Spain. Journal of Paleontology 71 (6), 1157–1171. https://doi.org/10.1017/S002233600003609X.
Vila, B., Sellés, A.G., Brusatte, S.L., 2016. Diversity and faunal changes in the latest Cretaceous dinosaur communities of southwestern Europe. Cretaceous Research 57, 552–564. https://doi.org/10.1016/j.cretres.2015.07.003.
Von Huene, F., 1914. Das natürliche System der Saurischia. Zentr. für Min., Geol. Palaeont., B 1914, 154–158.
Wang, S., Ding, N., Ma, W., Yu, W., Zheng, T., Choiniere, J., Xu, X., 2024. Convincing Evidence of Carnivorous Diet in Alvarezsaurian Dinosaur. bioRxiv 2024–12. https://doi.org/10.1101/2024.12.06.627300. Preprint.
Weishampel, D.B., Csiki, Z., Benton, M.J., Grigorescu, D., Codrea, V., 2010. Palaeobiogeographic relationships of the Haţeg biota—Between isolation and innovation. Palaeogeography, Palaeoclimatology, Palaeoecology 293 (3–4), 419–437. https://doi.org/10.1016/j.palaeo.2010.03.024.
Wilson, J.A., Sereno, P.C., Srivastava, S., Bhatt, D.K., Khosla, A., Shani, A., 2003. A new abelisaurid (Dinosauria, Theropoda) from the Lameta formation (Cretaceous, Maastrichtian) of India, vol. 31. Contributions of the Museum of Palaeontology of the University of Michigan, pp. 1–42.
Wings, O., Tütken, T., Fowler, D.W., Martin, T., Pfretzschner, H.U., Sun, G., 2015. Dinosaur teeth from the Jurassic Qigu and Shishugou Formations of the Junggar Basin (Xinjiang/China) and their paleoecologic implications. Paläontologische Zeitschrift 89, 485–502. https://doi.org/10.1007/s12542-014-0227-3.
Winkler, D.E., Kubo, T., Kubo, M.O., Kaiser, T.M., Tütken, T., 2022. First application of dental microwear texture analysis to infer theropod feeding ecology. Palaeontology 65 (6), e12632. https://doi.org/10.1111/pala.12632.
Xu, X., Li, F., 2016. A new microraptorine specimen (Theropoda: Dromaeosauridae) with a brief comment on the evolution of compound bones in theropods. Vertebrata PalAsiatica 54 (4), 153–169.
Zanno, L.E., Makovicky, P.J., 2011. Herbivorous ecomorphology and specialization patterns in theropod dinosaur evolution. Proceedings of the National Academy of Sciences 108 (1), 232–237. https://doi.org/10.1073/pnas.101192410.
Zanno, L.E., Gillette, D.D., Albright, L.B., Titus, A.L., 2009. A new North American therizinosaurid and the role of herbivory in 'predatory'dinosaur evolution. Proceedings of the Royal Society B: Biological Sciences 276 (1672), 3505–3511. https://doi.org/10.1098/rspb.2009.1029.
Zelenitsky, D.K., Therrien, F., Tanaka, K., Currie, P.J., DeBuhr, C.L., 2017. Latest Cretaceous eggshell assemblage from the Willow Creek Formation (upper Maastrichtian–lower Paleocene) of Alberta, Canada, reveals higher dinosaur diversity than represented by skeletal remains. Canadian Journal of Earth Sciences 54 (2), 134–140. https://doi.org/10.1139/cjes-2016-0080.

Appendix A. Supplementary data

Supplementary data to this article can be found online at https://doi.org/10.1016/j.cretres.2025.106199.